LASER INDUCED BREAKDOWN SPECTROSCOPIC ANALYSIS OF METAL AEROSOLS GENERATED BY PNEUMATIC NEBULIZATION OF AQUEOUS SOLUTIONS

A Thesis Submitted to
the Graduate School of Engineering and Sciences of
İzmir Institute of Technology
in Partial Fulfillment of the Requirements for the Degree of

MASTER OF SCIENCE

in Chemistry

by
Dilek ARICA ATEŞ

JULY 2010
İZMİR

We approve the thesis of **Dilek ARICA ATEŞ**

_____
Assoc. Prof. Dr. Şerife YALÇIN
Supervisor

_____
Prof Dr. Hürriyet POLAT
Committee Member

_____
Assist. Prof. Dr. Enver TARHAN
Committee Member

1 July 2010

_____
Prof. Dr. Serdar ÖZÇELİK
Head of the Department of Chemistry

_____
Assoc. Prof. Dr. Talat YALÇIN
Dean of the Graduate School of
Engineering and Sciences

ACKNOWLEDGMENTS

I would like thank to several people who really helped and supported me through out my thesis studies.

First of all, I would like to thank to Assoc. Prof. Dr. Şerife YALÇIN for her generous supervising through out the time that we were working.

Besides, I would like to show my great appreciation to Prof. Dr. Hürriyet POLAT for her valuable comments and great effort on particle size measurements. I would like to thank to Assist. Prof. Dr Enver Tarhan for his valuable comments.

Also, I would like to thank to my laboratory mates Semira ÜNAL and Nadir ARAS for their great friendship, help and for the enjoyable times we had together.

Nevertheless, I would like to mention my room mates Ezel BOYACI and Meral KARACA and Ayşegül ŞEKER for their companian, and especially to Esen DÖNERTAŞ, Merve DEMİRKURT, Hüseyin İLGÜ. They were the shining colors of my days. Also, Elif Bilge KAVUN has been a great companion for many years. Her sincere opinions and act have put on great challenge on me. She is the only one to be real sisters with.

We would like to give our appreciation to TÜBİTAK for the financial support for this project. (TBAG-108T376).

Furthermore, I would like to thank to Selahattin ÇAKMAK from Ege University Glass Workshop and Polat BULANIK for their great talent and patience on making the glass wares we needed.

Last but not least, I would like to thank to my friend, love, and husband, “my everything” Atilla ATEŞ for his valuable love and encouragement for completion of my thesis and overcoming my difficult days. Without him, life would not exist for me.

ABSTRACT

LASER INDUCED BREAKDOWN SPECTROSCOPIC ANALYSIS OF METAL AEROSOLS GENERATED BY PNEUMATIC NEBULIZATION OF AQUEOUS SOLUTIONS

Laser Induced Breakdown Spectroscopy, LIBS, is an analytical technique used to determine the elemental composition of samples in all forms. In this study, an experimental LIBS system has been designed and constructed for the analysis of metal aerosol particles that are generated by a pneumatic nebulizer. This research provides a basis and preliminary data for the construction of a portable LIBS system to analyze metals in aqueous environments.

The aerosol particles generated from the pneumatic nebulizer travel through a sample introduction unit to reach the sample cell in which they interact with the laser beam. The source of light is a Nd:YAG laser at 532 nm, 10 Hz. When the laser beam is focused inside the sample cell, plasma is generated, and the emission containing the spectral information about the sample being analyzed is focused onto the spectrograph and detected by a gated detector. The optimum optical and experimental parameters were systematically investigated.

The aqueous analyte solutions were prepared from their salts before introduced into the system. In this work, laser-induced breakdown spectroscopic emissions of Na, Ca, Mg and K aerosols were studied. In single shot mode, the minimum detectable aqueous concentrations were found as 250 ppb, 500 ppb, 400 ppb and 10 mg/L respectively. For 10 shot accumulated analyses in repetitive mode, based on 3σ criterion, the detection limit (LOD) was determined as 1 mg/L, 0.6 mg/L, 1.5 mg/L and 16.3 mg/L respectively. The efficiency of the drying unit has been evaluated by particle size measurements. It has been shown that the Na aerosols with particle size of 4.3 μm decreases to 0.5 μm after passing through the membrane dryer unit.

ÖZET

PNÖMATİK NEBULİZASYON METODU İLE SULU ÇÖZELTİLERDEN OLUŞTURULAN METAL AEROSOLLERİNİN LAZER OLUŞTURMALI PLAZMA SPEKTROSKOPİSİ İLE ANALİZİ

Lazer Oluşturmalı Plazma Spektroskopisi, LIBS, katı, sıvı, gaz örneklerin elemental bileşimlerinin belirlenmesinde kullanılan bir analitik metoddur. Bu tez çalışmasında, pnömatik sisleştirici tarafından üretilen aerosollerin analizi için bir LIBS düzeneği tasarlanmış ve kurulmuştur. Sisleştirici tarafından oluşturulan aerosol parçacıkları ısıtma/soğutma bölümü ve membran kurutucudan geçerek örnek hücresine ulaşmaktadır. Bu örnek hücresinde, parçacıklar ile lazer ışınının etkileşimi gerçekleşir. Işık kaynağı olarak 532 nm ve 10 Hz'de pulslu ışık veren Nd:YAG kristalli lazer kullanılmaktadır. Bu pulslu ışın, uygun optik malzemeler ile örnek hücresine odaklanır ve plazma oluşturulur. Oluşan plazma emisyonu spektrograf ve dedektör üzerine düşürülür ve spektal görüntü kaydedilir. Bu spektral dağılım, örnek hakkında bilgiler içermektedir.

Analit çözeltiler, katı metal tuzlarından hazırlanarak sisteme verilmiştir. Bu çalışmada, Na, Ca, Mg ve K elementlerinden elde edilen aerosollerin spektral emisyonları incelenmiştir. Tek vuruşlu analizlerde tayin edilebilir en düşük sulu çözelti konsantrasyonları sırasıyla 250 ppb, 500 ppb, 400 ppb and 10 ppm olarak bulunmuştur. Tekrarlamalı modda 10 vuruş toplandığı analizlerde ise tayin limiti 1 mg/L, 0.6 mg/L, 1.5 mg/L ve 16.3 mg/L olarak bulunmuştur.

Bunun yanısıra, kurutma bölümünün verimini değerlendirmek amacıyla parçacık ölçümleri gerçekleştirilmiştir. Sodyum aerosollerinin ısıtma/soğutma ve membran kurutucu bölümlerinden geçtikten sonra parçacık boyutunun 4.3 μm'den 0.5 μm'ye düştüğü görülmüştür.

TABLE OF CONTENTS

LIST OF FIGURES

Figure **Page**

LIST OF TABLES

Table **Page**

CHAPTER 1

INTRODUCTION

1.1. Subject

Everyday the amount of pollutants and toxic compounds are becoming more frequently used in industry and many other areas of work. In order to determine, identify and control those pollutants and toxic materials, atomic spectroscopic instruments like Atomic Absorption Spectroscopy, AAS, Inductively Coupled Plasma Optical Emission Spectroscopy, ICP-OES are required and widely used. However, due to long time of analyses the consumption rates of purge gasses and chemicals are high for those methods. Even more, the process steps accompanied to those methods to isolate the analyte may result as the loss of identity of the sample. Besides, all those methods require time to bring the sample to the laboratory. On account of those reasons described above, in order to save time and other expenses, a method should be developed for fast and cheap analysis compared to those methods. Laser Induced Breakdown technique provides many advantages such as no sample preparation and no chemical solvent consumption. Also, LIBS technique can be applied on all types of sample with high detection limits and precision of 5%. The benefits of the LIBS are further discussed in following sections.

This thesis presents a study on the development of a compact prototype device which can be used on field. The designed instrument is used for the analysis of several elements. After the optimization of system parameters are performed, real samples are introduced to the system.

1.2. Introduction to Laser Induced Breakdown Spectroscopy, LIBS

By the invention of lasers in 1960s, lasers have taken place in many areas of research (Andrew 2006). One of the applications of the laser includes the Laser Induced Breakdown Spectroscopy, shortly LIBS (Radziemski, Cremers, Wiley, 2006). LIBS is an atomic emission spectroscopic technique which uses a pulsed laser to form plasma. Plasma is considered to be a cloud of electrons and ions that results from the breakdown

of the sample. Laser plasma can be formed on any type of a sample: solid, liquid, gas and aerosol. When a high power pulsed laser sent onto the sample, the sample absorbs the energy from the laser; heated up, melts and evaporates. Due to the high peak powers of the laser, temperatures may reach up to 20.000 K. At that moment; the sample atomizes, ionizes and forms the plasma. Plasma is a luminous cloud that has time dependent characteristics. After the laser pulse is off, cooling process starts through the expansion of the plasma with a shockwave in front. During the plasma cooling, radiative emission of the light at characteristic wavelength of the sample is observed while excited atoms and ions relax back to the ground state. This atomic emission is monitored by a time resolved, gated detector.

In recent years, LIBS technique has been widely used in various areas: cultural heritage, space applications, environmental monitoring, industrial control, LIBS sensor applications, and is ever growing. This growth in the applications of LIBS emerges in parallel with the technological developments in instrumentation. In typical plasma spectrometers like ICP-MS, ICP-OES, temperatures are on the orders of a few thousands of Kelvins. However, with laser generated plasmas temperatures above 20000 K may be obtained. That provides a medium close to complete ionization and establishment of the local thermodynamic equilibrium.

1.3. Local Thermodynamic Equilibrium

In order to explain several plasma properties like degree of ionization, temperature and electron density, it is assumed that local thermodynamic equilibrium exists in plasma, so that the populations of energy levels and velocity of particles can be described in terms of temperature. It is assumed that equilibrium exists in small parts of space. The plasma is said to be at equilibrium and the temperature of the plasma is the same in every part of the plasma (Griem, 1964).

The populations in energy levels fit into the Boltzmann Equation shown in Eqn 1.1. For the calculations of the spectral temperature Boltzmann Equation can be used. Boltzmann eqn. relates line intensities, I_1 and I_2 to the ratio of the statistical factor g, transition probabilities, A and the wavelengths, λ of the upper and lower energy levels, E_2, E_1. If the plot of the ratio of the constants in the equation versus the energy in electron volt is drawn the slope of the best fitted line gives the spectral temperature.

$$\ln\frac{I_1}{I_2}=\ln\frac{g_1A_1\lambda_2}{g_2A_2\lambda_2}-(E_2-E_1)/kT \tag{1.1.}$$

The velocities of the species in plasma can be calculated by Maxwell Equation (Eqn 1.2). In Maxwellian Equations m is the mass of an electron, v is the velocity, k is the Boltzmann constant and T stands for the temperature.

$$f(v)=4\pi\left(\frac{m}{2kT}\right)^{3/2}v^2e^{-mv^2/2kT} \tag{1.2.}$$

In addition, the chemical composition of the plasma is explained by the Saha-Bolztmann Equation given in Eqn 1.3.

$$\frac{I_1}{I_2}=2\frac{g_1A_1\lambda_2}{g_2A_2\lambda_1}\frac{(2\pi mk)^{3/2}}{h^3}\frac{1}{N_e}T^{3/2}\exp\left[-\frac{\left(E_1+E_\infty-E_2-\Delta E_\infty\right)}{kT}\right] \tag{1.3.}$$

1.4. Advantages and Disadvantages of LIBS

There are advantages and disadvantages of this technique. First of all, LIBS technique has little or no sample preparation. This is an advantage because it eliminates possible contaminations and loss of analyte throughout the sample preparation steps. Besides, LIBS may be easily applied to all forms of samples, solid, liquid and gas. Even analyses of very hard samples are permitted. For solid samples depth profiling and lateral resolution is possible. This advantage arises from the fact that LIBS systems use only small amounts of sample. Craters with a few micrometers of diameters are obtained with suitable optics. By the help of the use of fiber optic cables, LIBS system can be applied as a remote analysis technique. Further more, the compact portable LIBS set-ups enable field analysis. One of the major advantages of LIBS is its speed and ability to make multi-elemental analysis. By using suitable spectrograph equipped with a multi channel detector, analysis of dozens of elements in a single laser shot may take just a second.

Contrary to the advantages of LIBS, there are some disadvantages. Since the energy of laser may vary from one shot to another, the response monitored changes. This 5-10% energy variation may lead to a problem during low level of quantification.

Therefore, in order to eliminate this disadvantage, several measurements may be averaged. Also, during the analysis of solids, the surface composition may be different than the bulk composition. Since the crater formed by the focused beam is just a few micrometers in size and depth, the investigated area may not be a representative of the whole sample. As a result of the above facts, the analytical figures of merit are not as good as the other widely used atomic spectroscopic techniques such as ICP-OES and AAS. The detection limits are in the range of hundreds of ppb, (μg/L), to ppm, (mg/L), levels, but are improved by new studies. Table 1.1 shows some of the detection limits from the literature.

1.5. Instrumentation

A LIBS set-up is typically composed of 3 main parts; *laser*, as the light source, *focusing optics*, to focus the laser to form the plasma and to collect the emission, and *detection unit* composed of a spectrometer and a detector.

The laser beam can be send on to the sample in two different directions regarding the plasma image position on the slit. The plasma image can be parallel or perpendicular to the slit height. By different orientations, the portion of the plasma falling onto the slit changes, thus the response.

Figure 1.1. shows a typical LIBS set-up (Caceres et al., 2001). Here, the sample is placed on a stage with a step motor. The beam from the laser sources are focused onto the sample on this stage. After the plasma formation, the emission is collected by a fiber optic cable which is connected to a monochromator and a detector. The triggering is controlled by the computer.

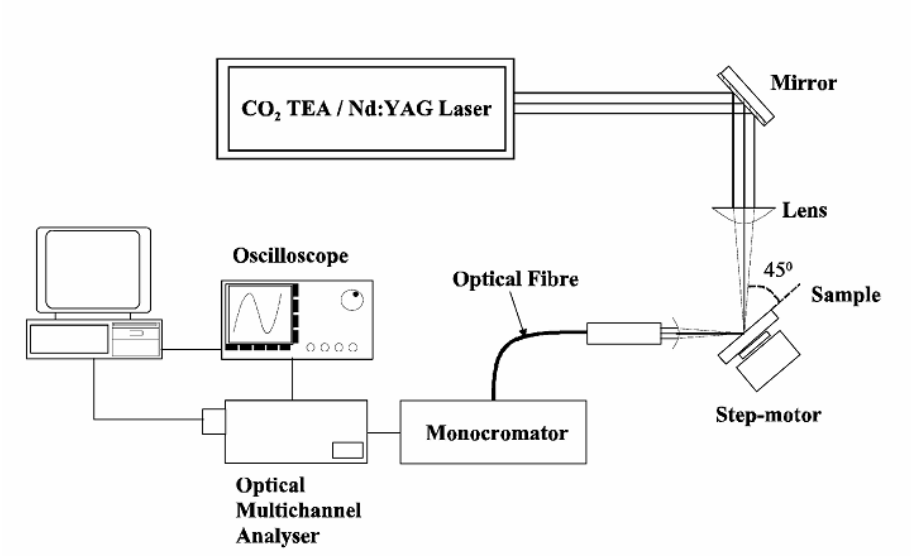

Figure 1.1. A typical LIBS set-up.

Harith et al. (2002) studies the set-up for LIBS analysis of water. In this study the laser is sent to bulk water surface at 60° incidence angle with respect to the sample surface. The emission is collected by a fiber optic cable. (Figure 1.2.) In this optical configuration the splashing of the water to the optical components was prevented.

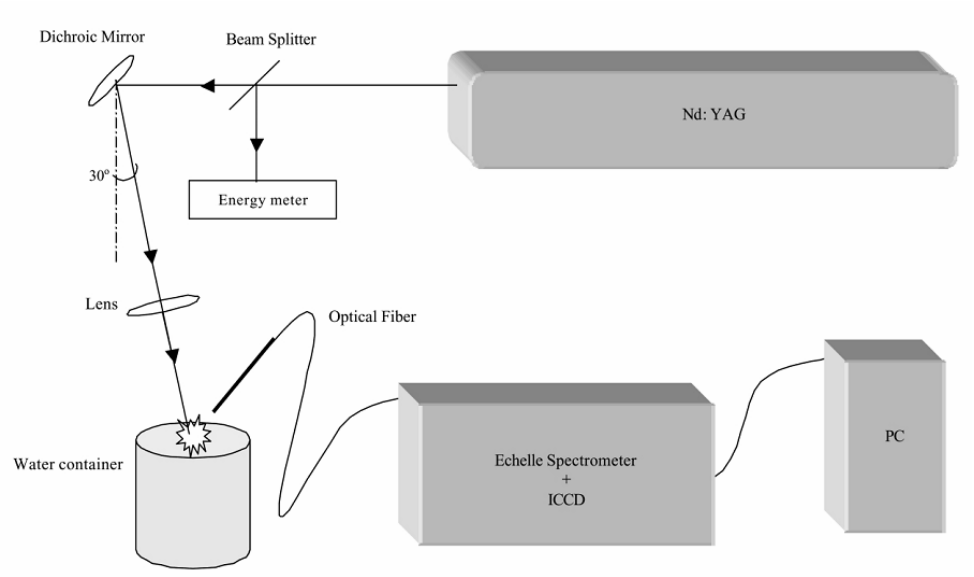

Figure 1.2. LIBS set-up for liquids. Beam focused on surface of the liquid.

1.5.1. Lasers

50 years after the first demonstration of lasers at Hughes Research laboratories, lasers are used not only in scientific purposes but also in a wide range of fields; medicine, industry, military and many more.

LASER is an acronym standing for *light amplification by stimulated emission of radiation* (Andrew 2006). Laser beam is formed by the lasing action inside the optical cavity. The lasing action starts by the pump sources. The active medium absorbs the energy from those pumping sources and becomes excited. This stimulated emission travels through two highly reflective mirrors at two sides of the medium. The stimulated emission moves through these two mirrors for many times and becomes intensified. Then, the beam exits the media from the partially transparent mirror when it reaches equilibrium. Figure 1.3. shows the optical cavity of a laser.

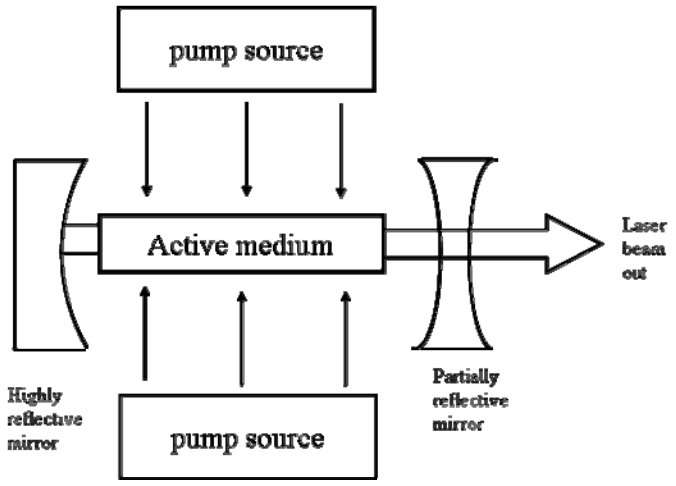

Figure 1.3. Optical cavity.

Lasers produce photons which are coherent, monochromatic, and directional. The absorption of energy leads to transition of electrons from ground state E_1 to the excited state, E_2. The energy difference is represented as in Equation 1.4.

$$\Delta E = E2 - E1 = \frac{hc}{\lambda} \tag{1.4.}$$

In Equation 1.1, it's shown that the energy difference between the ground state and the excited state is related with h, Plank constant, c, speed of light and λ, the wavelength of

the characteristic emission. Relaxation forms a radiation which is called *stimulated emission* which represents the coherency, the same phase in space and time. Lasers are the source of light amplification by the help of the stimulated emission.

Boltzmann distribution which represents the population of atoms in possible energy levels is given in Equation 1.5.

$$\frac{N_2}{N_1} = \frac{g_1}{g_2} \quad e^{-\Delta E / KT} \tag{1.5.}$$

N_2 stands for the population in the upper and lower energy levels. g is the statistical weight of upper level, E is the upper state for emission and k is the Boltzmann Constant ($1.38 * 10^{-38}$ J/K). When N_1 is more than N_2, more energy levels are included; the emission can take place in two or more levels.

There are different types of lasers varying on their active media or pump sources and can be listed as solid state lasers, gas lasers, dye lasers and semiconductor diode lasers. Only Nd:YAG laser as an example to solid state lasers will be presented under the interest of this work. Some other examples of solid state laser other than Nd:YAG laser are Cr:YAG and Nd:YLF. For the gas lasers, the active medium is composed of gases and is pumped by electrical charges. He-Ne and CO_2 lasers are some examples. Dye lasers imply an active medium of dyes. Likewise, semiconductor materials such as gallium arsenide and gallium nitrate are used in semiconductor lasers.

1.5.1.1. Nd:YAG Lasers

Neodymium-doped yttrium aluminum garnate, Nd:YAG, lasers are the most commonly used and understood solid state lasers (Andrew 2006).

The pumping sources are the flash lamps whose energy is enough to excite the atoms of the crystal. At each time the flash lamps are fired the active medium will emit a light at a wavelength of fundamental emission, 1064 nm. On the other hand, by the use of an optical device, harmonic generator, light emissions from near IR to UV region at wavelengths of 532 nm, 356 nm, and 266 nm can be obtained as the second, third and fourth harmonics, respectively.

When the absorption and emission energies are the same it is called a two level laser system. Nd:YAG lasers which are four-level lasers are more efficient compared to three or two level laser, because the excited state energies (E) are much higher than the ground state, so does the population (N) in forth level.

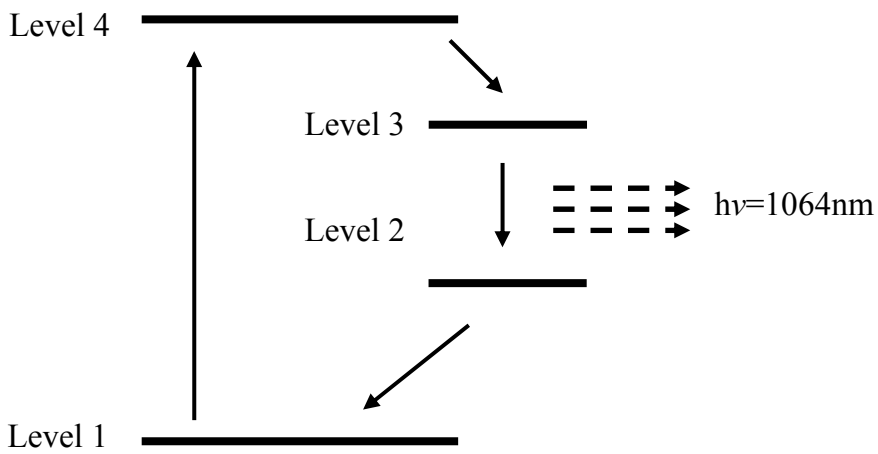

Figure 1.4. A four level laser scheme.

1.5.2. Optic Materials

All the optical materials used in LIBS set-ups should be specially designed for the wavelength of the laser beam. The mirrors are used to direct the laser beam coming out of the active medium. They are front surface coated and reflect the beam at 99.9 % reflectivity. The focusing lenses focus the laser beam onto the sample spot to form the plasma. In the same manner, the collecting lenses make the emission of the plasma parallel and focus on the slit of the spectrograph. The diameter and the thickness of the lenses are important to match the requirements of the detection system and eliminate optical aberrations.

Besides to the lenses fiber optic cables are also used to manage the light because they are easy to handle. They are mostly preferred in portable systems (Laserna et al., 2008) and when the detection part of the system cannot get too close to the emission part (Cremers and Radziemski, 2006).

1.5.3. Detection

The light emission from the plasma is collected and sent onto the spectrograph using mirrors, lenses and/or sometimes transferred by fiber optics cable. In LIBS systems usually the detection section is composed of a monochromator or polychromators coupled with charge couple devices or photo multiplier tubes. Echelle type polychromators are multi channel spectrometers. Echelle type polychromators are more advantageous for the LIBS detection because, it enables the observation of a wide range of spectrum from a single laser shot. The presence of both a prism and a grating inside an Echelle type polychromator enables better dispersion of the emitted light. The dispersed emission is mostly detected by a charge coupled device (CCD), in which timing is possible and multi element analysis may be achieved simultaneously. Besides CCD's, photomultiplier tubes may be more useful for LIBS sensor applications.

1.6. LIBS on Liquid Samples Analysis

1.6.1. Direct Liquid Analysis

The literature work of Radziemski et al. in 1984 is one of the pioneering work on laser induced breakdown spectroscopic analysis of liquids. In this study, the laser spark has been directly formed on the liquid sample. This work has shown several fundamental skills for LIBS studies. The analyte signal has decreased as longer delay times are assigned. The broadening of lines is observed at early delay times. They have also observed relatively high limit of detection for several elements.

One of the advantages of Laser Induced Breakdown Spectroscopy is that, it can be directly applied onto the sample. Analysis of liquids can be done directly onto the surface as well. Koch et al. (2004) has investigated the chromium in liquid samples. Laser beam has been sent into the sample container horizontally and the emission is collected from the top of the sample container. In this work, different concentrations of chromium samples have been analyzed. The limit of detection has been found as 200 ppm. But it has been declared that the sensitivity is low due to the quenching in liquids.

Another study given by Huang et al. (2006) is on analysis of aluminum ions (Al^{+3}) in liquid droplets. This work has been about using electrospray ionization technique to produce droplets of aluminum salt solution by applying voltage onto the

nozzle of the flow injection system. The aluminum salt solution has been preconcentrated on ion-exchange column, before the nozzle. The laser beam has been focused onto those droplets at the tip of the nozzle. This work has claimed that the preconcentration has made an advantage on LIBS system.

Yaroshchyk et al. (2005) has given a comparison work of LIBS using liquid jets and static liquids. This work shows most of the disadvantages of working with liquids such as splashing and bubble formation on the surface of liquid samples. They have shown that the liquid jets, in which the sample is thrown from a plastic funnel, is more rapid and easy to acquire data than as in static liquid.

Caceres et al. (2001) has demonstrated a different methodology of LIBS for quantitative analysis of trace metals in liquids. In this work, Al and Na ions were determined in liquid samples that have been converted to ice by freezing in liquid nitrogen. Low background levels have been obtained. The detection limits for Al and Na has been declared as 1 ppm and 2 ppm respectively.

Gondal et al. (2007) has studied on determination of poisonous metals in paint factories. Similar to the above work of Caceres, paint sample has been filtered and dried at 105°C. Then LIBS analysis has been carried out. They have shown that the results of LIBS and ICP are similar to each other.

Janzen et al. (2005) has presented a novel HPLC-LIBS hyphenated technique. In this method, first the sample is separated molecularly by HPLC and then by a piezoelectric nozzle the separated specie is transferred to droplets. Later, each droplet is analyzed by the laser focused onto the system. The data collection is accomplished by Paschen Runge Spectrometer coupled with 31 PMTs to detect 31 different elements, simultaneously. The voltage applied on the piezoelectric can be altered to form droplets with different sizes. In this work the diameters of the droplets generated has been declared as 50 to 100 μm. Yet, in this study the authors has been faced with the difficulties working with liquids. They have shown that the bulk liquid analysis has some disadvantages such as very rapid decay of the plasma (approximately 1 μs) and bubble formation occur on the surface analysis of liquids by LIBS.

In general, LIBS analysis of liquids directly on the surface or in bulk suffers from several obstacles, such as shockwave formation, bubble formation, splashing of the sample and scattering of the laser beam. These difficulties have some negative effects by reducing the data quality and hence the detection limit of the technique. In

order to eliminate these problems several approaches may be performed such as use of multiple pulses, aerosol formation or chemical derivatization. (Unal et al., 2010)

1.6.2. Double Pulse LIBS

In order to obtain better emission signal intensities double laser pulses may be used in analysis of liquids. Both of the lasers strike onto the sample, with a time difference between the pulses. The first pulse usually heats and pre-ablates the sample. On account of the enhanced ablation in double pulse LIBS the emission signals obtained are in better spectral quality. Hahn et al. (2006) has demonstrated use of dual pulse in analysis of aerosols and gases. The energy of the second pulse (290 mJ) they have used was more energetic than the first one (100mJ/pulse) thus the plasma formed by the second plasma were larger than the initial plasma. Their aerosol particles have been carried by air to the sample cell. This study has given an example of the dual pulse application on aerosols. The signal enhancements have been given as 4 fold.

Yoshiro et al. (1996) had experiments to determine the iron suspensions in water by LIBS using two sequential lasers. The limit of detection has been highly improved by the use of two sequential lasers. It has been found as 16 ppb for single pulse excitation. By two sequential lasers, the particles in a liquid sample can be detected. Furthermore, it has been declared that in limit of detection studies, other parameters such as pulse energy, timing of two lasers are important.

1.6.3. LIBS on Aerosol Samples

Aerosol formation is an alternative method in liquids analysis by LIBS. Aerosols can be generated by either a pneumatic nebulizer or an ultrasonic nebulizer.

One of the initiative works by Radziemski et al. in 1983 was the analysis of air aerosols by LIBS. Beryllium, sodium, arsenic and mercury elements have been detected in air. In this work the samples were introduced to the nebulizer/heater chamber. The temperature has been above 100 °C. Air concentrations have been calculated for beryllium. The air concentration of beryllium, 0.6 ng/ g air corresponds to solution concentration of 40 ng/mL. Also, in this work LIBS technique has been compared with ICP and it has been declared that the detection limits of ICP results are much lower than the LIBS concentrations.

Another work of Radziemski et al. (1988) gives another example for use of pneumatic nebulizer in the analysis of cadmium, lead and zinc aerosols. They have collected the aerosols on the filter and flame atomic absorption spectrometry method has been used to see the mass of lead accumulated on filter. On the other hand, high concentrations of samples have generated large particles and since the energy is fixed the entire sample may not be fully atomized. They have also proved that the response of lead analyte has been increased by addition of sodium element into the solution.

Moreover, the article by Cheng et al. (2000) has given an example of detection of chromium by forming aerosols. Despite to the other studies, this time the aerosol particles are generated by an atomizer. The diameter of the particles are measured and found out to be 2.4 μm (± 1.5 μm). The detection limit for chromium in air has been found as 4000 ng/m^3. Besides, they have sought for the effect of laser wavelength and found out that the lowest signal-to-noise ratio is calculated for 266 nm. They have expressed the importance of laser energy for ionization of the analyte.

Panne et al. (2001) has also demonstrated an alternative way of analysis of aerosols. In their work they stabilized the lead aerosols on filters in an automatic system. Quartz fibers have been used as filtering medium. They have analyzed several toxic elements such as Cd, Ni, As, Co, Mn, Sb, Cr, Tl, Sn, V, Cu and Pb. This method can be taken as a model for detection of heavy metals in environment. They have provided detection limits in air concentrations and amount of analyte per area of filter paper. As the authors declare, deposition of particles on filters has brought advantage in achieving better detection limits.

Also, Hahn et al. (2001) has developed an aerosol system for aerosol generation and calibration by LIBS. They have used a pneumatic nebulizer and formed submicron sized particles. They have placed a porous plate on top of the nebulizer and a co-flow of the nitrogen is introduced to the system. Then the aerosols travel to the six-way sample chamber. They have investigated the particle size of iron and titanium oxide particles by TEM (Transmission Electron Microscopy). The range has been determined as 13.2 to 9.5 nm (±7 nm).

In addition, Hahn et al. (2001) has shown on-line analysis of aerosol particles in air. They have detected magnesium, aluminum, calcium and sodium on a holiday period in town. They have used a commercially available air sampling system which produces particles less than 10 μm in diameter. The particles formed by this inlet are introduced

to a four-way sample cell. The cell is connected to a vacuum pump at one arm and at another arm the laser is focused into the sample. Also by the help of a pierced mirror the plasma emission is collected back to a spectrometer. They have also investigated the particle sizes of the particles. They were in the range of 0.1 to 1.0 μm. They have found that since the fireworks are used more on holidays the particle distribution is found out to be more. The mass concentrations in air are given as 46 ppt for aluminum, 0.65 ppb for sodium and 0.21 ppb by mass for calcium on holidays.

Besides to all the above works, in literature there are some applications of portable LIBS systems. One of them has been presented by Laserna et al. in 2003. Their study was about a portable LIBS system for rapid on site analysis of steel. A probe composed of laser with both focusing and collecting optics has been focused onto the sample. The emission is transformed by fiber optic cable. In addition to the field analysis, they have also demonstrated the same analysis in lab conditions with the same probe design.

For the demonstration of particle-plasma interactions, Hohreiter and Hahn (2006) show the non-homogeneity of the plasma of calcium particles. In this study the aerosol particles are formed by a pneumatic nebulizer purged by HEPA filtered air. The particle size distribution and shape of the aerosols have been determined using optical microscopy. At different delay times plasma images are collected. At late times the plasmas have been difficult to make qualitative analysis.

In another study by Hahn et al. (2007) pneumatic nebulization technique has been used to generate particles of sodium and magnesium. The carrier gas used was air filtered by HEPA filter. The particle sizes of the particles have been expected to be less than 100 nm regarding to the TEM (Transmission Electron Microscopy) analysis. They have also shown that addition of elements like copper, zinc or tungsten enhances the analyte signal intensity. The additional elements cool down the plasma so that the analyte signal gets higher. This piece of work is valuable in order to understand the particle-plasma interactions.

In 2008, Laserna et al., this time, has worked on a stand-off design for the detection of liquid aerosols. The LIBS plasma formed was at 10 meters distance. The laser has been focused onto the particles on top of the nebulizer needle. High standard deviation of the measurements leads to uncertainty yet the authors claim that the limit of detection for sodium element is 55 ppm. The sizes of the particles generated are in size range of 4 to 16 μm for 1000 ppm sodium particles. They have also shown that the

aerosol concentration should not be so low, if so, the data does not represent the sample and poor data is obtained. If the sampling rate is so high, then the laser beam cannot penetrate through the aerosol particles.

Table 1.1. gives several examples from the literature and the declared detection limits.

1.7. Aim of the Study

Many important elements which may be toxic or hazardous for the environment need to be controlled in real time, on-line. Most frequently the instruments used for the identification and determination of those elements are time-consuming, difficult to conduct and require using high amount of sample or chemicals.

Regarding the advantages of the LIBS technique, such that the analysis provides no sample preparation and the identity of the sample is not changed the sample can be directly analyzed by LIBS. For that reason, a portable LIBS system can be designed, constructed and optimized for the determination of the elements present in environmental samples, both qualitatively and quantitatively.

Due to the obstacles faced on direct liquid LIBS analysis, this thesis focuses on the conversion of the liquid sample into aerosols. In this work, an aerosol generation system has been constructed and equipped with the commercially available parts. In the second part of the work, qualitative and quantitative analysis have been shown. Also, the detection limits will be discussed with the relevant studies from the literature.

Table 1.1. Detection limits from literature.

Element	**LOD**	**Ref**	**Method**	**Notes:**
Na	0.0091 %w/v	Onge et al	Saline solutions	Flowing and nonflowing surface analysis
	1.6mg/L	Aglio et al	Double pulse – bulk liquid	
	8 mg/L	Chadwick et al	Liquid jet	
	33300 mg/m3	Molina et al	Elements present in different ratio of gases	No quantification
	1 mg/L	Lin et al	ESI	Matrix effect. Same cation (K) different anions Solutions prepared with water&methanol (1:1)
	173 mg/kg	Gondal et al		Calibration with powder form of the analyte//residues of liquid sample collected
	0.08 ug/ml	Harith et al	water	
Mg	0.2 ug /g	Gautier et al	Double Pulse/ Alloy	Lasers oriented at different geometry
	0.5ug/g		Single Pulse / Alloy	
	34 ug/L	Lazic et al	Bubble cavity	
	5 mg/L	Aglio et al	Double pulse – bulk liquid	
	0.4 mg/L	Chadwick et al	Liquid jet	
	0.21 mg/L	Lazic et al	Double pulse	
	200mg/kg	Gondal et al		Calibration with powder form of the analyte//residues of liquid sample collected
	1 ug/ml	Harith et al	Water-	panaromic
	3.19 mg/L	Mohamed et al.	Aluminum alloy	
Ca	0.4 mg/L	Chadwick et al	Liquid jet	
	301 mg/kg	Gondal et al		Calibration with powder form of the analyte//residues of liquid sample collected
K	28 mg/kg	Gondal et al		

15

CHAPTER 2

EXPERIMENTAL

2.1. LIBS Experimental Set-up

In this work a lab-made system has been designed, constructed and used for the analysis of metal aerosols. The set-up may be divided into three sub categories. The first step involves the generation of the aerosols; the second part is the heating/cooling and drying unit for desolvation of the aerosols before entering into the sample cell. The last part is the detection system in which spectral line intensities of the metal aerosols are monitored.

2.1.1. Aerosol Generation

The pneumatic nebulizer used in our measurements throughout this study is given in (Fig 2.1). After small amount of sample has been placed inside the nebulizer (7 mL), pressurized N_2 gas has been applied from the bottom. The gas leaving the orifice of the nebulizer converts the liquid sample into fine aerosol droplets. The liquid sample has been divided into sub-droplet particles by the effect of the gas flowing at 3.5 mL/min. The uptake rate of the nebulizer is calculated to be 0.255mL/min at gas flow rate of 3.5 mL/min. The nitrogen gas used from the nitrogen generator (NitroFlow) was with 98.3% purity. The gas flow rate has been monitored by a flow meter (Cole Parmer).

Figure 2.1. Medical used to convert aqueous solutions into aerosols.

2.1.2. Desolvation of the Aerosols

The solvent content of the aerosols should be removed to form clear, stable and lowest possible plasma size and to eliminate instrumental and spectral interferences.

2.1.2.1. Heating/Cooling Unit

The aerosols formed by the pneumatic nebulizer have been traveling through a glass tube fitting on top of the exit of the nebulizer. This glass tube is wrapped by heating tape (Cole Parmer) and the temperature inside the glass heating tube has been increased to 110 °C. This temperature has been chosen in order to evaporate the solvent, which is water. After the heating unit, the hot aerosols and the purge gas have been moving into the mini condenser, which is connected to a cooler circulator (PolyScience) adjusted to 4 °C. Here, the evaporated solvent has been condensed and collected at the end of the cooling unit. Much of the drain has been collected from this heating/drying unit. This compact unit (Figure 2.2.) has been constructed at Ege University Glassware Workshop. The efficiency of the heating/cooling unit has been determined using Atomic Absorption Spectrometry (Therma Elemental Solaar AA Spectrometer). Drains of 10 ppm Cu^{2+} solution have been collected. The results show that the analyte concentration present in drain is 1 ppm. This shows that, 90% of the analyte is transported to the sample cell while 10% is lost to the drain during the desolvation process.

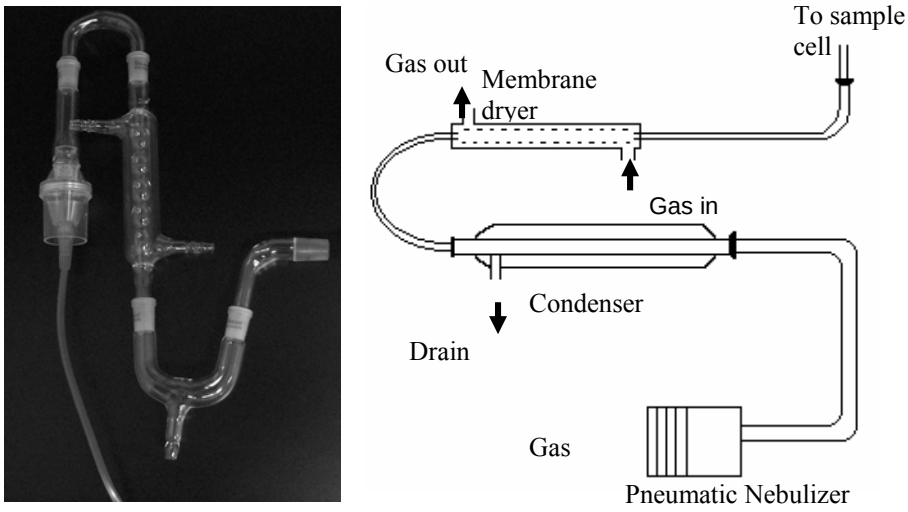

Figure 2.2. The pictorial and schematic representation of the heating/cooling unit.

2.1.2.2. Membrane Drying

After the heating/cooling unit, the aerosols have been going through a naphion membrane dryer (Perma Pure PD50). The naphion structure is selective to water. (What's Naphion?® Perma Pure LLC). Here, the aerosols have been dried by a countercurrent flow of drying gas (nitrogen) with respect to sample flow. The excess moisture has been given out of the membrane dryer. In order to test the removal of the moisture content of the aerosols in the membrane unit, silica gel beads have been placed at the exit of the membrane drying gas. The color change of the silica gel beads from blue to pink was indicating the removal of water content of the aerosols. At last, the dry aerosols enter the sample cell.

2.2. Instrumental

All of the materials used are specially manufactured for LIBS systems. A Q-switched Nd:YAG laser (Quanta-Ray Lab-170, Spectra Physics) has been used as the laser source working at second harmonics, 532 nm. The laser pulses have 10 ns duration at 10 Hz repetition rate. The laser beam has been reflected by the highly reflective mirrors (coated, 532 nm reflective, New Focus,) towards the sample cell. The lens used to focus the laser beam has 5 cm focal length and 1 inch outer diameter (Thorlabs). The collimating lenses used to collect the plasma image onto the spectrograph were in 5 cm and 17.5 cm focal length (Thorlabs). The energy of the incoming laser beam has been measured by a power meter head (Nova II, Ophir, Israel). The teflon sample cell, with five arms, each 1 inch outer diameter, has been designed in our group previously (Unal et al 2009) and manufactured in a local machine shop in Urla, İzmir. The arms at which the laser beam entering the cell and the emission to be collected are covered with quartz windows. The medium inside the sample cell have been kept uniformly flowing using a vacuum pump (Edwards) connected to a third arm of the sample cell. The plasma image has been focused onto an Echelle type spectrograph (Mechelle 5000 Andor Inc.) coupled with an ICCD detector (iStar DH734, Andor Inc.). The delay time (t_d) is the time that the detector gets on and starts data acquisition. The gate width (t_g) determines the amount of time that the detector collects light. The delay time (t_d) and gate width (t_g) have been optimized for each of the elements separately. All the system specifications have been summarized in Table 2.1.

Two different experimental LIBS set-up configurations have been constructed in this work which are horizontal and telescopic beam set-up. Horizontal beam set-up is the configuration in which the laser beam travels horizontally with respect to the optic table, entering the sample cell from the side arms. The telescopic beam set-up is the configuration in which the laser beam enters to the sample cell from the top, perpendicular to the optical table. The horizontal (a) and telescopic (b) beam set-up designs are shown schematically in Figure 2.3.

The size measurements of the aerosol particles have been accomplished by Malvern MasterSizer HD-2000 present at İYTE Chemistry Department. The aerosols have been introduced to the instrument exactly the same way as in aerosol generation system discussed above.

(a)

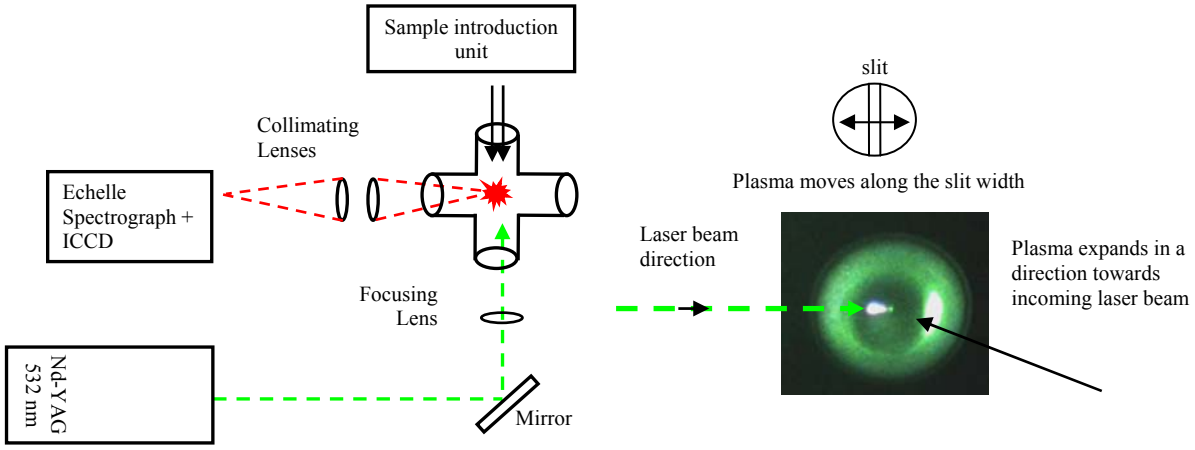

(b)

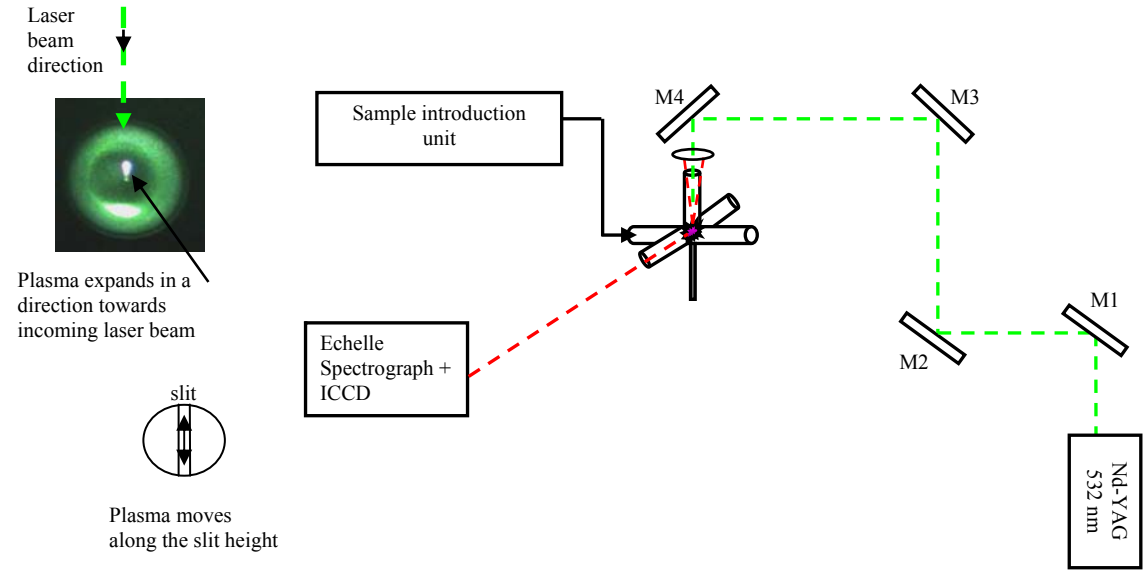

(c)

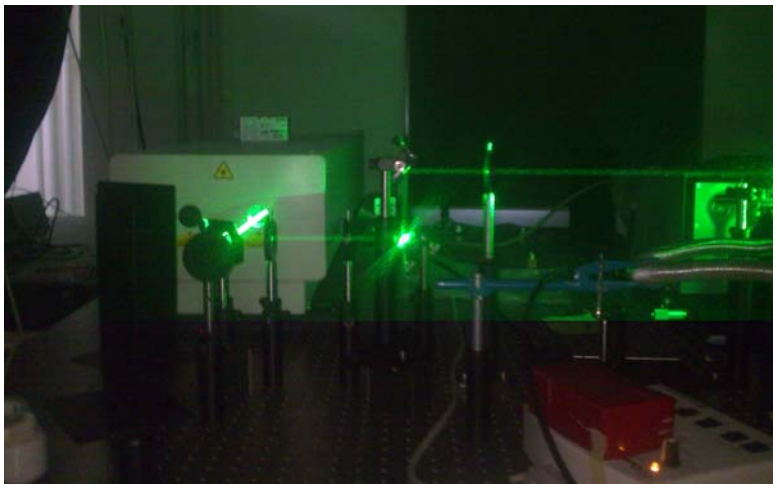

Figure 2.3. Horizontal (a) and telescopic (b) beam setup, (M: mirror). (c) Pictorial representation of the telescopic beam set-up.

Table 2.1. LIBS system specifications.

Q-switched Nd: YAG laser	Quanta-Ray Lab-170, Spectra Physics (California-USA)
Power meter	PE50BB-DIF-V2, Nova II, Ophir (Israel)
532 nm reflective mirrors	1″ OD, coated, 532 nm reflective (New Focus, Darmstad-Germany)
Focusing lens	5 cm (1″ OD, Thorlabs)
Collimating lenses	5 cm (1″ OD, Thorlabs) 17.5 cm (1″ OD, Thorlabs)
Echelle spectrograph	Mechelle 5000, Andor, f/7 (European)
ICCD detector	iStar DH734, Andor Inc. (European)
Pneumatic nebulizer	Medical Nebulizer
Heating-cooling unit	Handmade glassware
Heating tape	Cole Parmer, cloth insulated
Cooler	PolyScience Standard Digital Model 9106
Sample Cell	5-way handmade Teflon
Vacuum Pump	Edwards
Membrane Dryer	PermaPure PD-50 Naphion
Quartz Windows	1″ OD quartz
Nitrogen Genetaror	NitroFlow Lab
Flow Meters	Cole Parmer

2.2.2. Detection System

Through out the experiments an Echelle type spectrograph coupled with an ICCD type detector has been (resolution λ=0.4 nm) used. An echelle type spectrograph provides good resolution (wavelength coverage between 200-900 nm) with an added benefit of multi-element capability. The resolved wavelengths have been detected by 2-D array ICCD camera. With an ICCD camera rapid data acquisition with nanosecond time windows can be achieved. Time resolved measurements allow plasma emission to be monitored at different times of the plasma decaying. Suitable delay times and gate widths have been found from the systematical investigation of the decaying laser plasma at the specific analyte peaks. Usually after 4 μs of delay times the ICCD orders have been eliminated.

2.3. Reagents

Throughout the experiments fresh solutions have been prepared from the analytical grade solid salts of the metals; such as sodium chloride (Riedel), anhydrous calcium chloride (Fluka), magnesium chloride (Riedel) and potassium chloride (CarloErba) using ultra pure water (18Ω).

The nitrogen gas used to purge through the pneumatic nebulizer and naphion membrane dryer has been obtained from NirtoLab nitrogen generator at 98% purity.

For the multi element analysis a real sample of mineral water (KULA) has been used. Before the analysis, the mineral water has been kept in ultrasonic water bath for 5 minutes for degassing. Then the sample is directly introduced into the system. Also, tap water from the laboratory has been used for the multi-element analysis as well.

2.4. Aerosol Size Measurements

For the particle size measurements of the aerosols generated, the aerosol generation unit has been attached to MALVERN MasterSizer HD 2000 (Figure 2.4.). The gas flow rate, heating/cooling unit temperatures have been kept the same as in the LIBS analyses. The aerosols generated are given into the instrument. The aerosols are kept in continuous flow inside the quartz cell of the particle sizer in which the Mie Scattering occurs. By the help of this scattering on aerosol samples, the percent

distributions are obtained. In the second part of the size measurements, the membrane dryer has been attached at the exit of the aerosol generation unit. The effect of membrane dryer on particle size has been studied.

Figure 2.4. The aerosol generation unit attached to the particle sizer.

CHAPTER 3

RESULTS AND DISCUSSION

In this work, a LIBS system has been designed and constructed from its commercially available parts to monitor the LIBS signal of nebulized salt aerosols; NaCl, $CaCl_2$, $MgCl_2$ and KCl. The construction of the LIBS system and functions of each component has been discussed in detail, in Chapter 2.

There are some experimental and instrumental parameters to be optimized before obtaining representative LIBS spectra. The experimental parameters may be listed as the nebulizer flow rate and membrane dryer gas rate. The instrumental parameters are laser energy, delay time, gate width and gain.

3.1. Experimental Parameters

The experimental parameters refer to the variables that may be optimized regarding the aerosol generation part of the experimental set-up. These are the flow rates of sample and membrane dryer gas.

3.1.1. Effect of Sample Flow Rate on Signal Intensity

The sample flow rate is the actual gas flow rate applied from the bottom of the nebulizer to generate and transfer aerosol particles from the nebulizer to sample/plasma cell. During our measurements sample gas flow rate has been optimized. For this purpose LIBS signal measurements have been performed at different gas flow rates between 2.3 and 3.5 L/min.

As it can be seen in Figure 3.1, the signal intensities of the resonant sodium lines 588.9 and 589.6 nm increase as the flow rate increases, due to increased amount of aerosols carried into the sample cell. For this study, the optimum flow rate has been found as 3.5 L/min. 2.3 L/min is the minimum flow rate required to observe LIBS signal. Below this value there has been no sample transferred to the sample cell. Flow rates higher than 3.5 L/min. resulted with the removal of the gas tubing from the

nebulizer due to an increased amount of gas pressure. Therefore, the highest sample gas flow rate has been selected as 3.5 L/min. In addition, flow rate higher than 3.5 L/min has resulted with the generation of a high amount of aerosol particles and the plasma induced inside the sample cell has been highly moving. This movement was leading plasma image to be larger and to move more on the slit of the spectrograph. This situation might cause spectral and analytical disadvantages. The movement of the plasma image on slit may lead to distortions of the image. Besides the plasma image part which is left outside the slit, may reduce the analyte signal. For the later reasons, the experiments have been done successively, on the same day, using vertical beam set-up. In addition, a vacuum pump has been connected to one of the arms of the sample cell, to prevent overloading of aerosol particles inside the sample cell. A constant flow of aerosols have been accomplished inside the sample cell by the suction, and the pressure inside has been checked by a gauge control. The pressure inside the sample cell has been kept at atmospheric pressure.

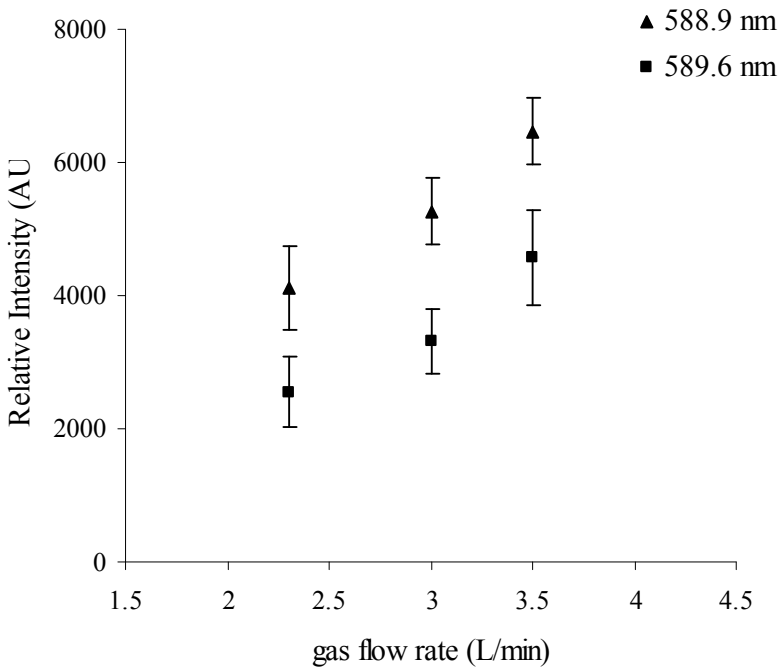

Figure 3.1. Effect of gas flow rate on Na signal intensity (50 ppm Na, 60mJ laser pulse energy, t_d=5μs and t_g=1ms have been used with 10 shot accumulation).

Besides, the amount of aqueous solution converted into aerosols is measured. First, 5 mL of sample is placed in the pneumatic nebulizer and after 2 minutes the volume of the remaining solution is measured using precise lab pipettes. Figure 3.1

shows the volume of aqueous salt solution converted into aerosol at different gas flow rates. The maximum amount of sample is converted into aerosol particles at the experimental carrier gas flow rate.

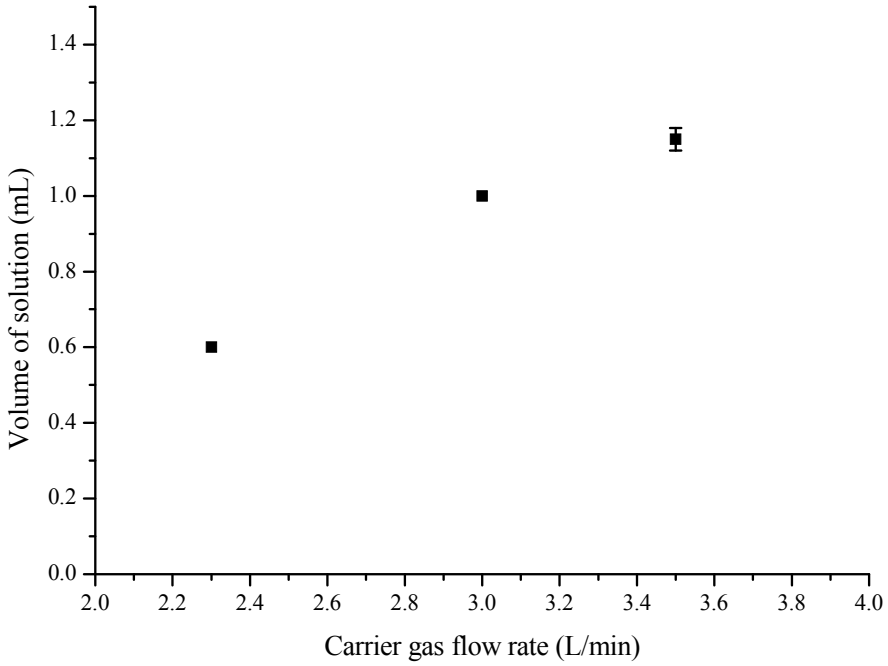

Figure 3.2. The amount of aqueous sample solution converted to aerosols at different carrier gas flow rates.

3.1.2. Drying Gas Flow Rate

The membrane dryer flow rate is the amount of gas flowing from the outside walls of the membrane in opposite direction with respect to the sample flow and is optimized with respect to the sample gas flow rate. As it is mentioned in the working principles of the membrane dryer, the drying gas flow should be kept below the sample flow rate; otherwise the desolvation process through the membrane can not be effectively achieved. 3.5 L/min drying gas flow rate has been used throughout the experiments. The same gas, from the nitrogen generator, has been used for both the sample flow and the drying gas flow.

3.2. Instrumental Parameters

Instrumental parameters are the variables that are related to the spectroscopy part of the system. They are listed as laser energy, delay time, gate width, and gain.

3.2.1. Effect of Laser Pulse Energy on Signal Intensity

Laser pulse energy is an important parameter in laser produced plasmas. The size, temperature and hence the extent of ionization is very much dependent on the laser pulse energy. This laser pulse energy is the source of energy for evaporation, atomization and ionization of the aerosol particles when it is focused inside the sample cell.

The variation in LIBS signal intensity as the energy of the incoming beam increases is shown in Figure 3.3. In Figure 3.3(a) laser pulse energy has been optimized with respect to peak heights of the Na(I) lines, 588.9 and 589.6 nm, whereas in Figure 3.3(b) 279.5 nm line of magnesium was investigated. In general, signal intensity increases as the pulse energy increases for both elements, however, a drastic increase in signal intensity after 50 mJ/pulse laser energy has been observed for Na. At laser pulse energies higher than 70 mJ/pulse, Na line intensity does not increase linearly that might be associated with the self absorption effect that is generally observed in laser plasmas. Therefore, 60 mJ/ pulse laser energy was chosen as optimum laser energy for the rest of the measurements for sodium. Similar results have been observed for Mg line as in sodium element case.

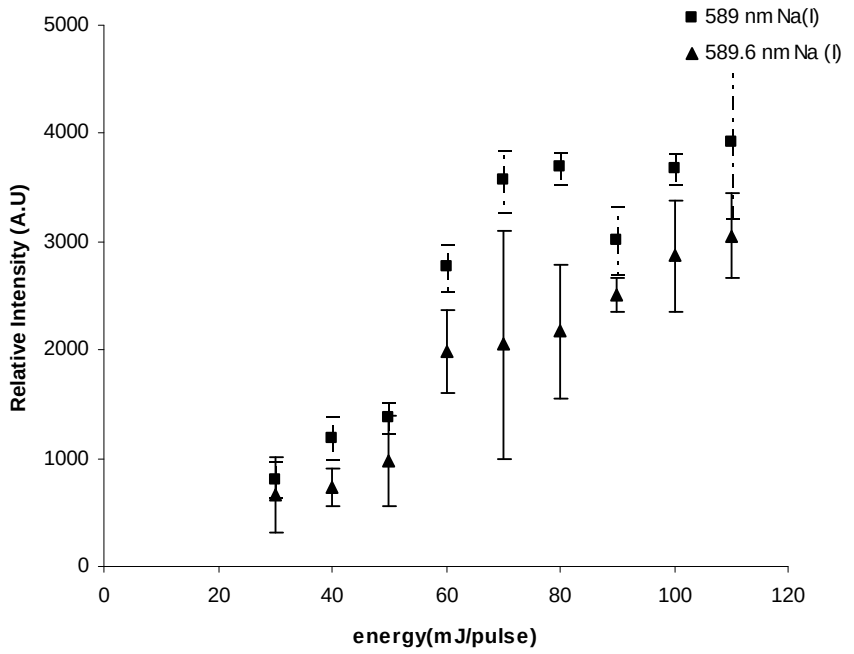

(a)

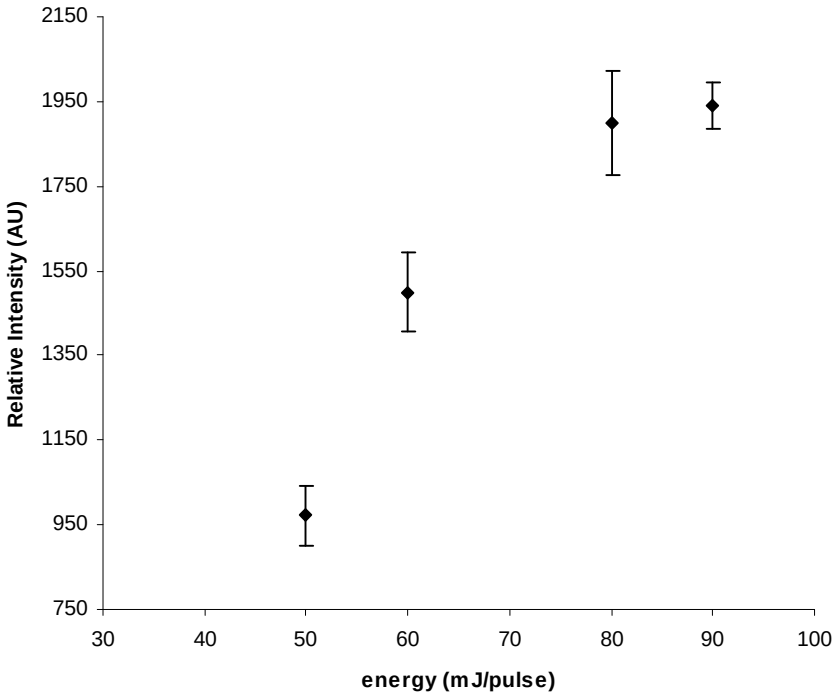

(b)

Figure 3.3. LIBS signal intensity variation of (a) 588.9 nm and 589.6nm Na(I), (b) 280.2 nm Mg(I) and (c) 766.6 nm K(I) lines with respect to laser energy **(continued on next page).**

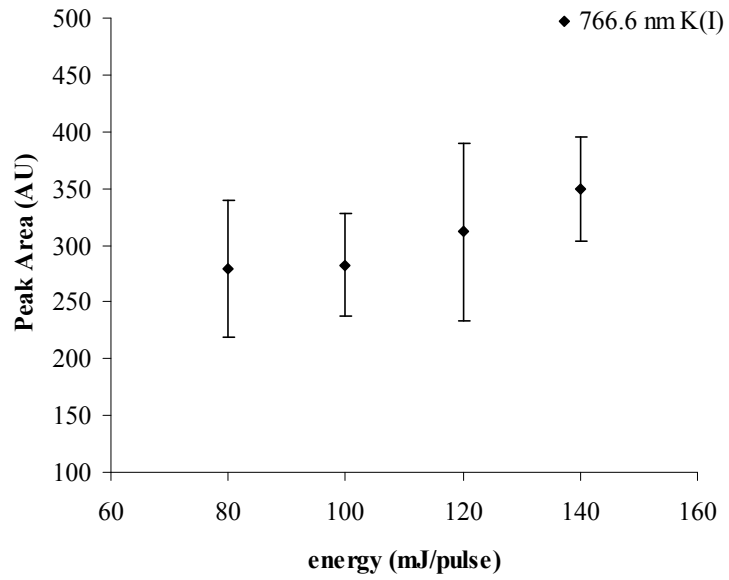

(c)

Figure 3.3. (cont) LIBS signal intensity variation of (c) K(I) 766.6 nm line with respect to laser energy.

Increasing the laser energy also increases the signal intensity; on the other hand, increase in laser energy has also increased the noise. Figure 3.4. shows the background peaks which appear near the analyte potassium signal at 766.6 nm.

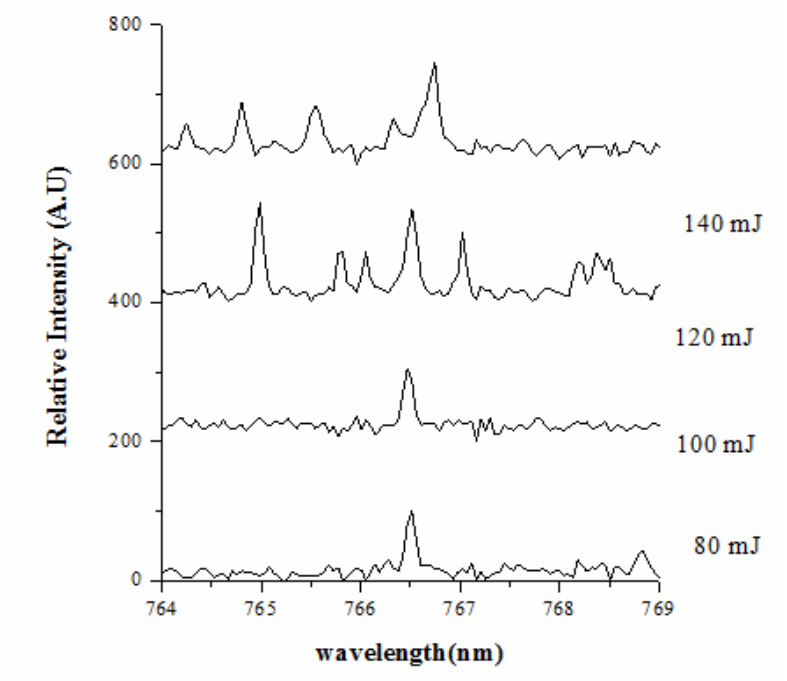

Figure 3.4. Appearance of noise with increasing laser energy. 766.6 nm K(I) line spectra obtained from single laser shot.

3.2.2. Time Resolution

Time resolution has great importance for the acquisition of the data at the correct instant. Delay time (t_d) and gate width (t_g) are the two timing options that need to be optimized.

Usually, in order to get rid of the structured and highly noisy spectra due to the continuous background emission at early times, late delay times on the orders of 4-5 μs have been preferred. Gate widths from hundreds of microseconds to several milliseconds are possible depending on the lifetime of the species under investigation.

Figure 3.5 shows time resolved spectra for calcium element. It is observed that before 4μs and after 8μs delay times no appreciable signal intensity was observed for 393.3 nm Ca line. Therefore, 4 μs has been selected as optimum delay time for calcium measurements.

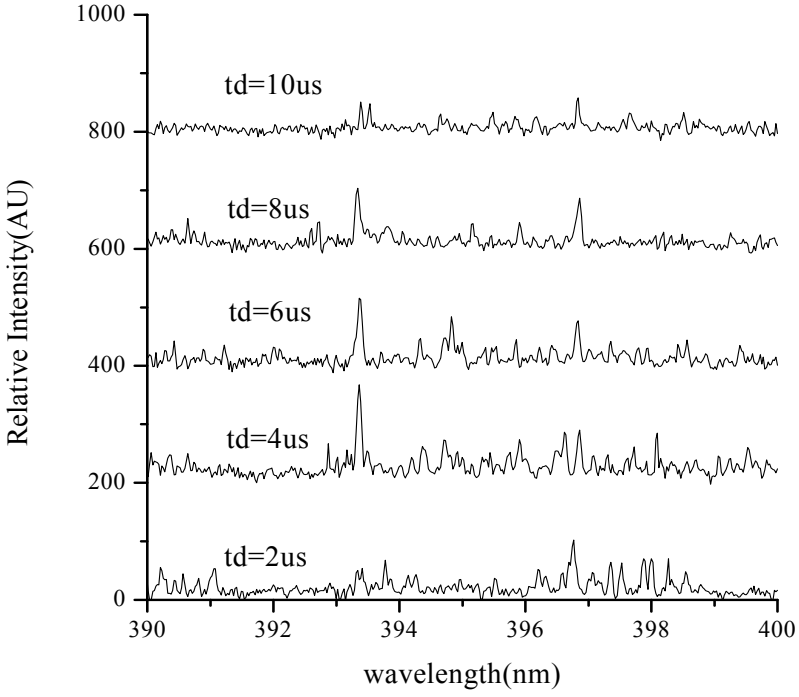

(a)

Figure 3.5. Time resolution for (a) Ca aerosols. t_g=2us, laser energy 100 mJ/pulse
(b) Time resolution for Na aerosols. t_g=1ms, laser energy 60 mJ/pulse
(continued on next page)

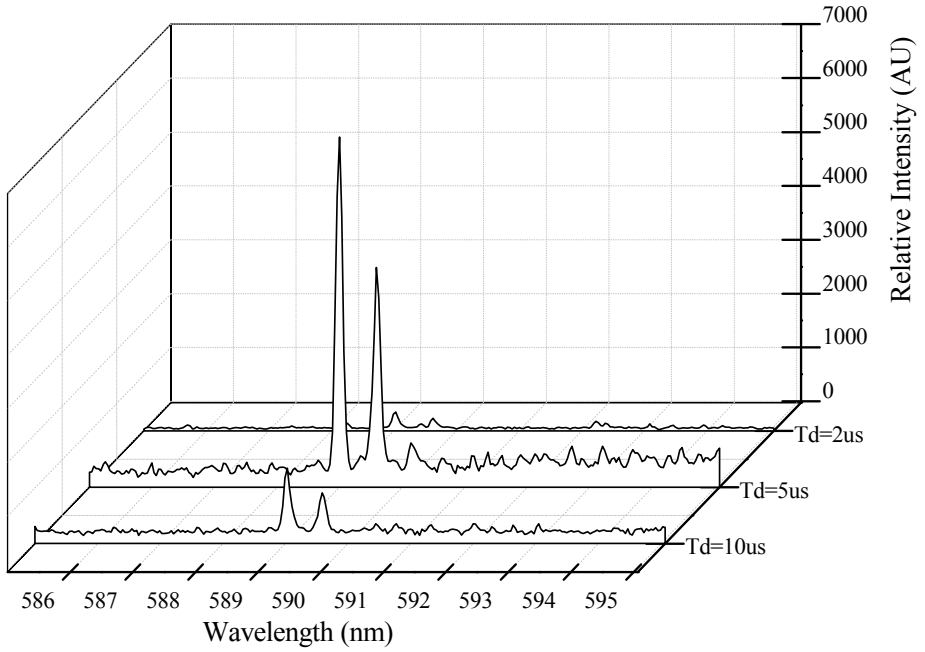

(b)

Figure 3.5. (cont) Time resolution for Na aerosols. t_g=1ms, laser energy 60 mJ/pulse

Gathering spectral information at the early times of the spectra may lead to spectral order lines to appear. These giant orders due to the presence of high background depress the presence and appearance of the analyte peak. Figure 3.6 shows the spectral quality of the early plasma, when 10 mg/L sodium solution is aspirated into the system, gate width at 2ms.

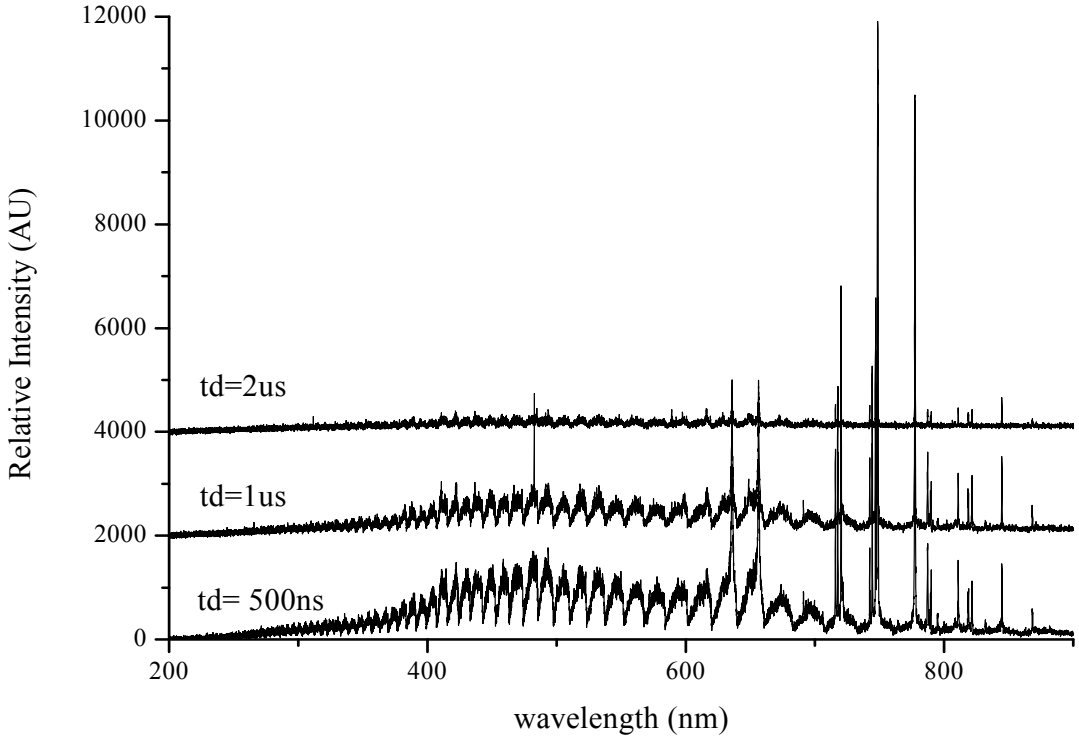

Figure 3.6. Spectra of early plasma. Laser energy 60mJ, gate width 2 ms.

3.2.3. Detector Gain

Another instrumental parameter to be considered is the gain applied on the detector. Gain is the numerical quantity related with the potential applied across the multichannel plate and affects the number of counts of photoelectron (Andor Technology, 2003).

The effect of gain applied to the detector has shown its importance to reveal the analyte peak from the high background. Figure 3.7 shows the effect of gain on 10 ppm K^+ solution aspired into the system. As it can be seen from the figure, a barely observable K signal at 766.6 nm with 100 gain becomes easily observable with a drastic enhancement at the gain of 200.

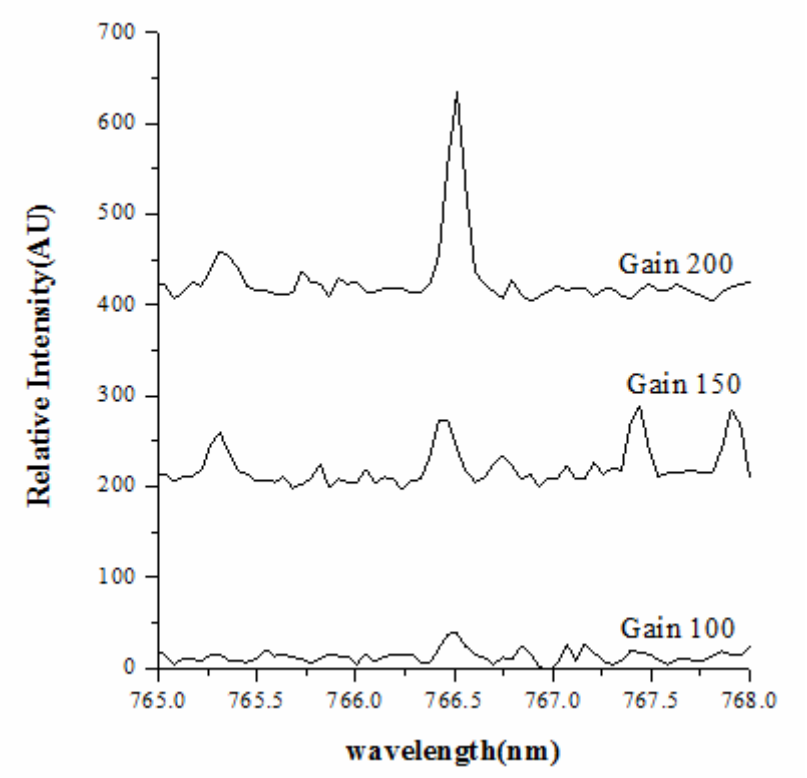

Figure 3.7. Effect of gain on potassium aerosols. t_d=4μs, t_g= 5μs, laser energy 140 mJ.

3.3. Qualitative Analysis

The LIBS spectra include qualitative and quantitative information about the sample being analyzed. The characteristic peaks are observed as a function of spectrometer resolution for qualitative analysis.

3.3.1. Representative Spectra

The representative LIBS spectra for sodium, calcium, magnesium and potassium emissions have been depicted Figure 3.8., 3.9., 3.10. and 3.11. respectively. The most probable resonance transitions of each element at 588.9 nm and 589.6 nm for sodium, 393.3 nm and 396.8 nm Ca, 279.5 nm for Mg have been observed with baseline separation. In each spectra, hydrogen line at 656.3 nm coming from the moisture content of the metal aerosols was clearly observed.

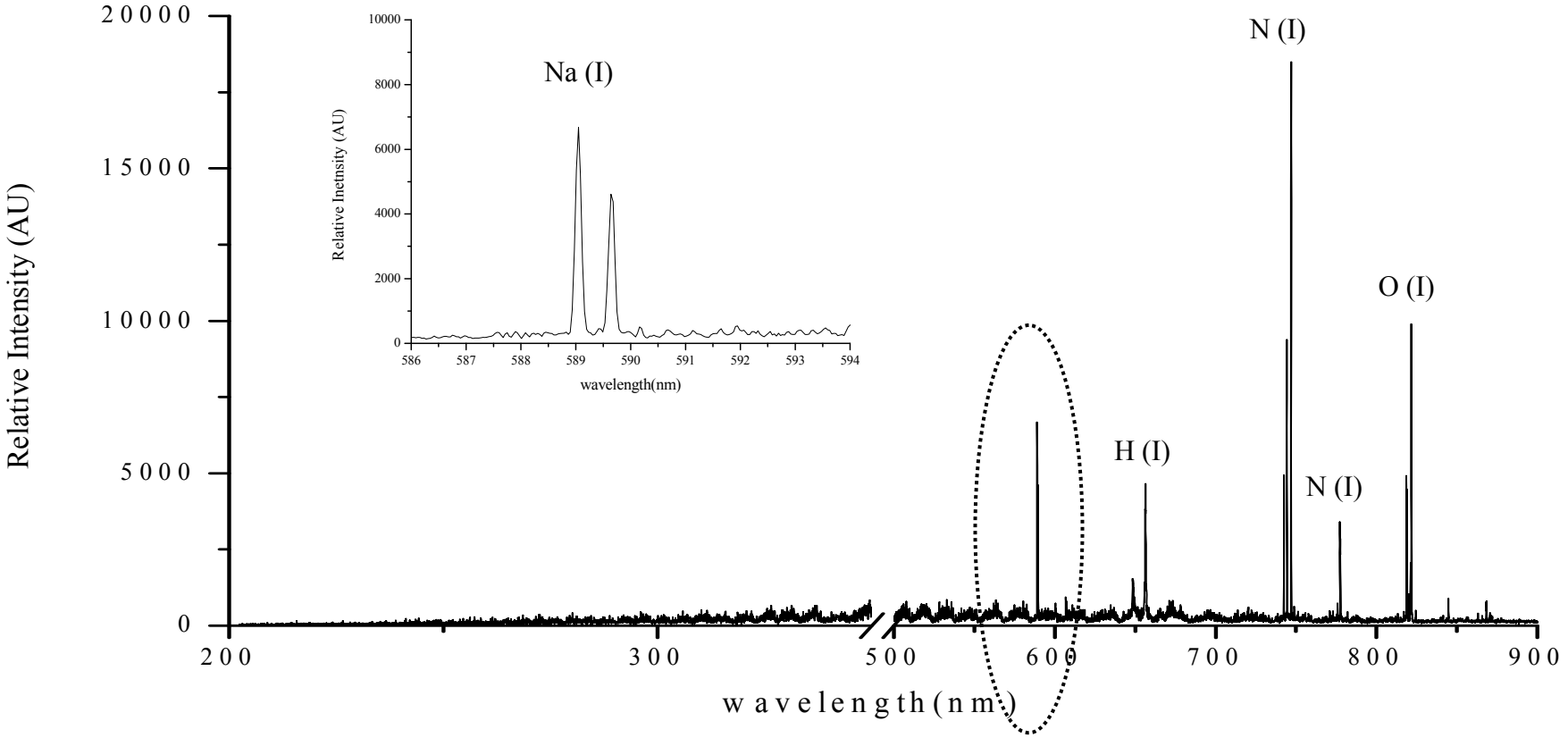

Figure 3.8. Representative Na spectra for 100 ppm Na at t_d= 5 us t_g=1 ms, laser energy=60 mJ (10 shot accumulation)

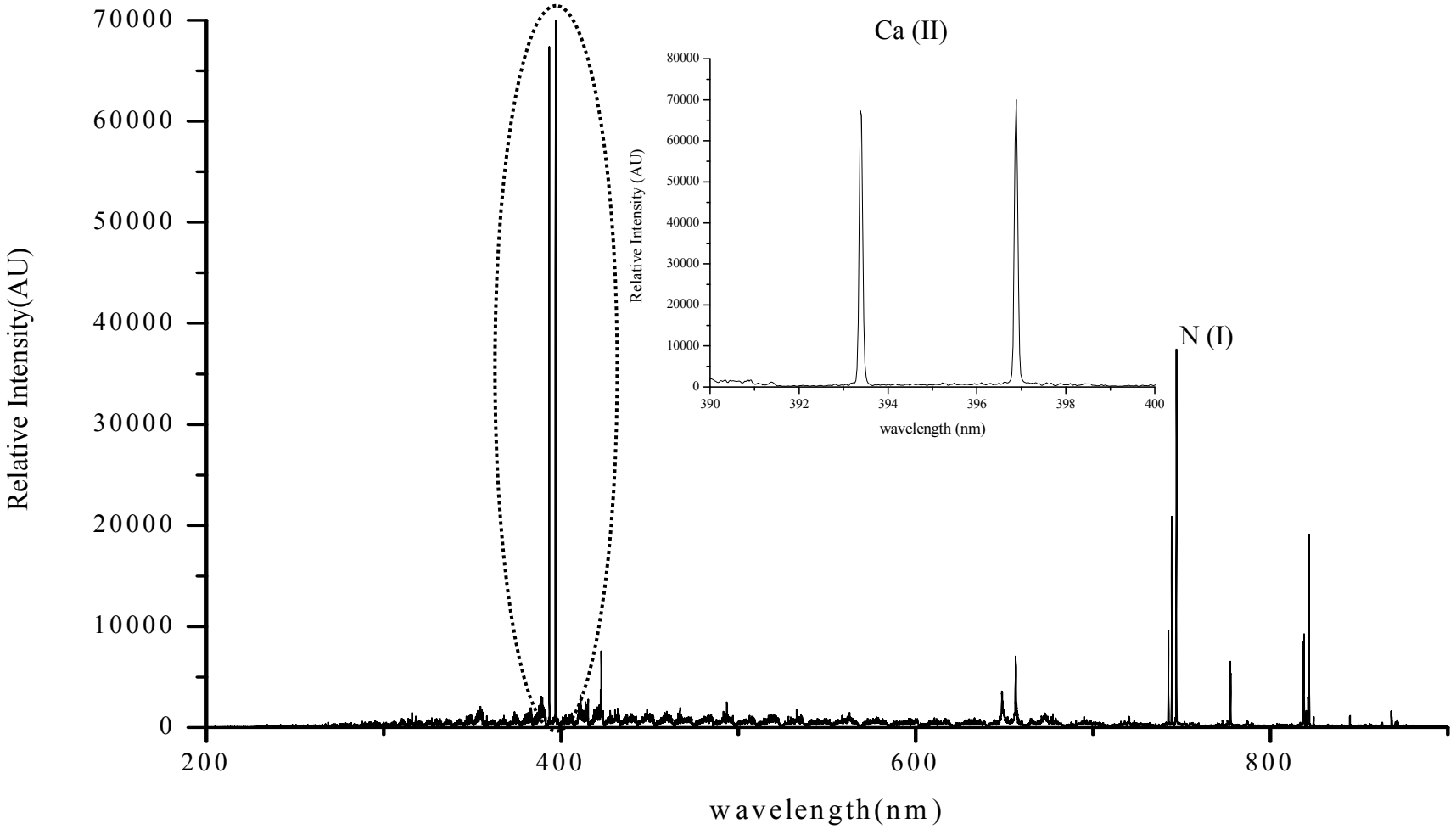

Figure 3.9. Representative Ca spectrum for 100 ppm Ca at t_d= 5us t_g=10us, laser energy=80 mJ (10 shot accumulation)

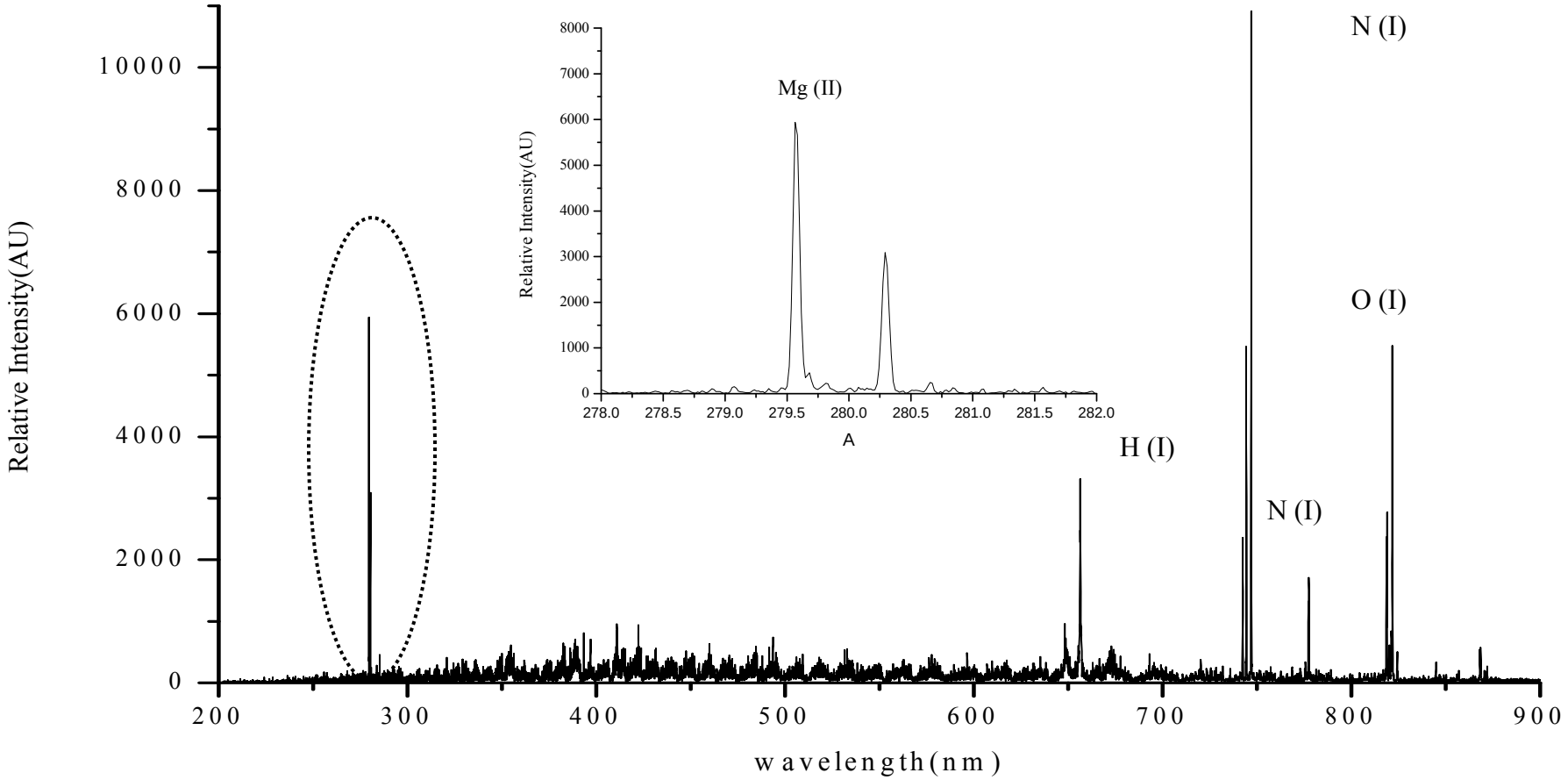

Figure 3.10. Representative Mg spectrum for 100 ppm Mg at t_d= 5 μs t_g=100 μs, laser energy=80 mJ (3 shot accumulation)

36

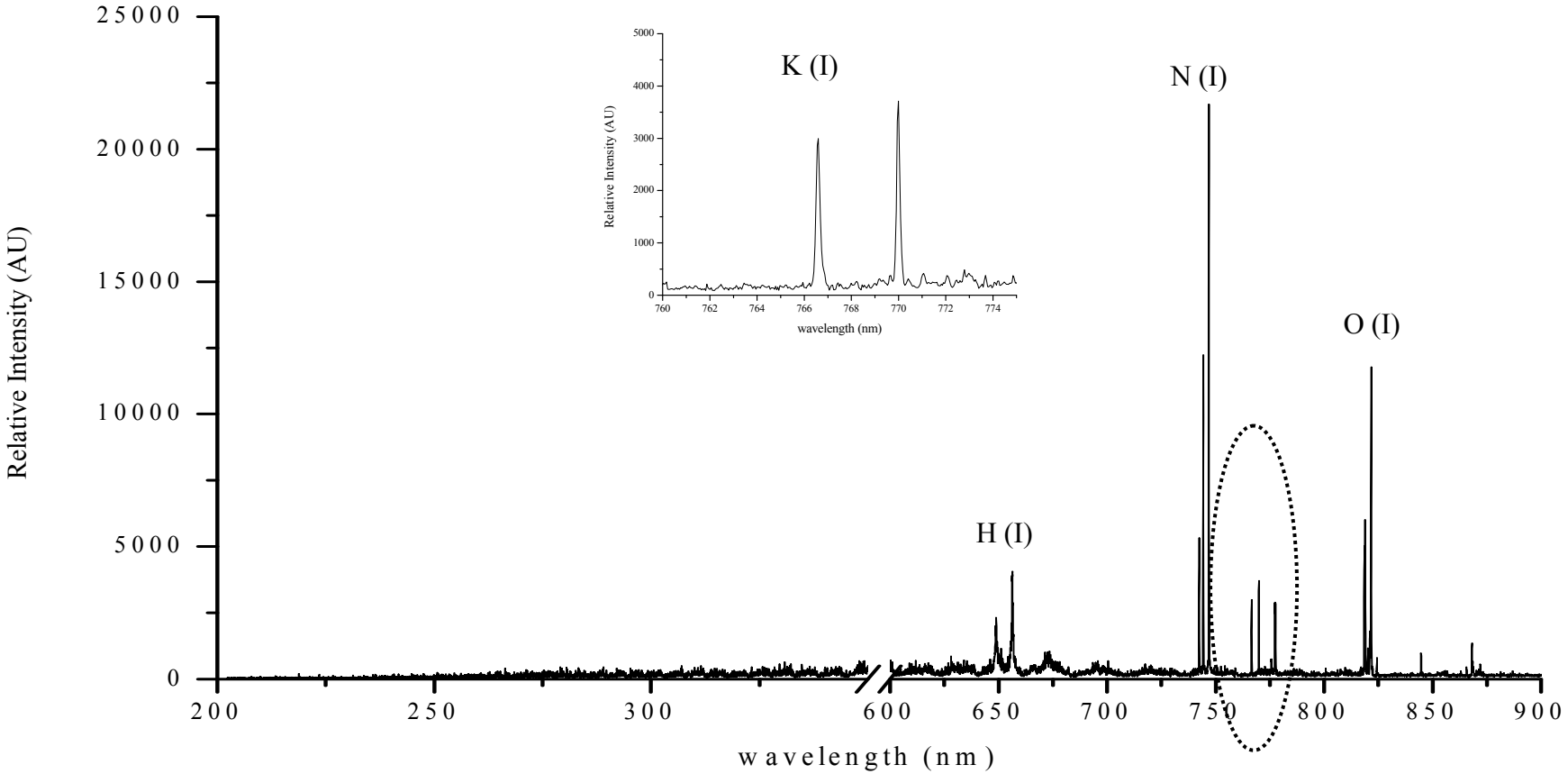

Figure 3.11. Representative K spectrum for 1000 ppm K at t_d= 5 4s t_g=500 μs, laser energy=140 mJ. (10 shot accumulation).

3.3.2. Effect of Membrane Dryer on H-α Line

The membrane dryer made up of naphion is selective to moisture content of the sample flowing through. The sample has been dried by a countercurrent flow of a membrane drying gas, and has been given out of the naphion membrane. The humidity of the gas coming out of the membrane dryer has been checked by placement of blue silica gels on the exit of the drying gas. The blue color of the silica gel (containing Cobalt salt) (Tekkim Blue Silica Gel) has changed to pink, in few minutes of analysis.

As Figure 3.13 indicates the use of membrane dryer has also decreased the background and especially the dominant H_α line (656.3 nm) has become lower in intensity. This was advantageous to reveal the analyte signal as shown in Figure 3.12. The intensity of the Na(I) 588.9 and 589.6 nm lines have increased when the membrane dryer is attached to the aerosol generation unit.

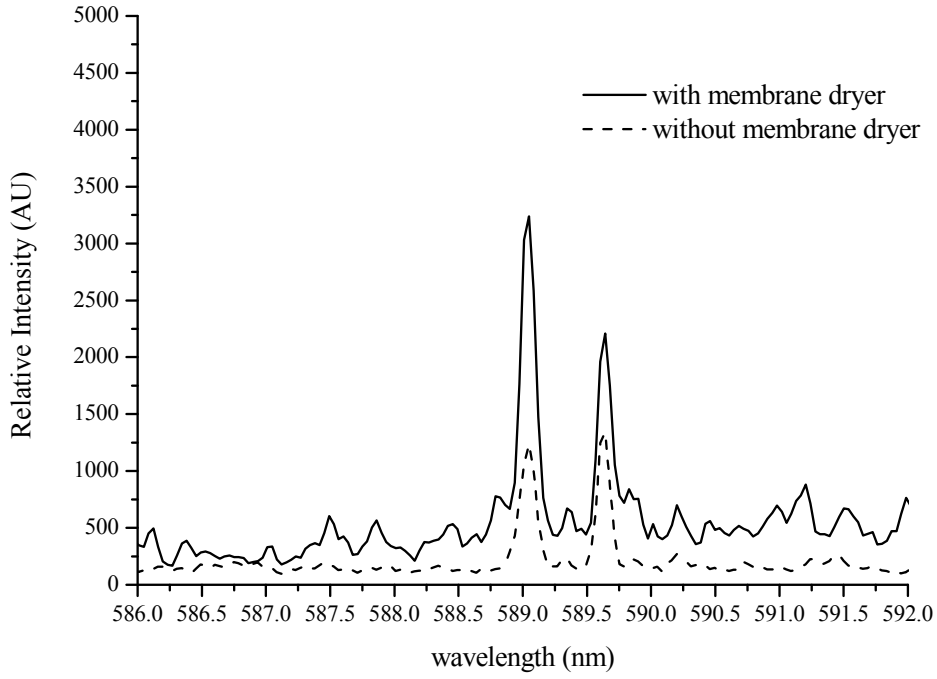

Figure 3.12. The decrease in intensity of 588.6 and 589.6 nm Na(I) line when membrane dryer is used.

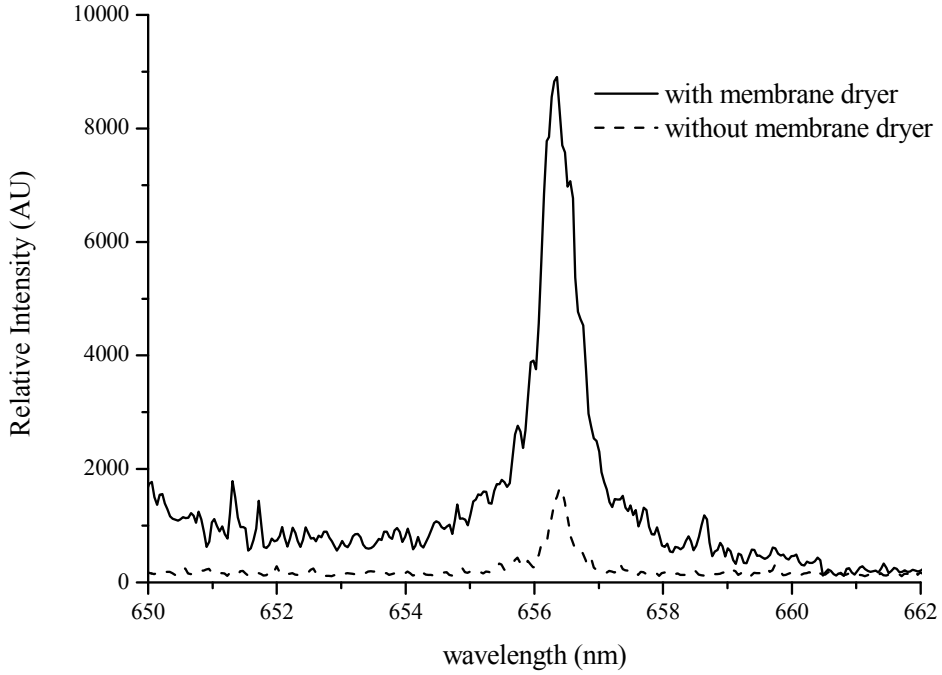

Figure 3.13. The decrease in intensity of 658.3 nm H line when membrane dryer is used.

3.3.4. Effect of Dessicant Prior to Membrane Dryer

A small glass adaptor has been placed between the exit of the heating/cooling unit and entrance of the membrane dryer. Inside, blue silica gels have been tucked in. At the end of several respective measurements, the color of the blue silica gel has turned to pink. This has been tried with 750 ppb Ca^{2+} solution. It has been observed that the peak areas of ionic calcium lines (393.3, 396.8 nm) and oxygen line (777 nm) have increased slightly. On the other hand this adaptation has been avoided because after a while the accumulation of analyte on silica may occur. Thus, it is not favored and not used in any other experiments. Table 3.1 shows the slight increase in average peak areas of 10 consecutive measurements.

Table 3.2. The icrease in peak area for Ca(II) 393.3 nm line when a dessicant is placed at the exit of the heating/ cooling unit.

Relative Intensity (AU)	Ca(II) 393.3 nm	O(I) 777 nm
Without dessicant	185 (±19.3)	128 (±42.7)
With dessicant	292 (±45.8)	297 (±46.9)

3.4. Quantitative Analysis

In order to show the applicability of the developed system for the quantitative analysis of the aqueous metal salts, the strongest emission lines of the analyte have been chosen to be monitored. These spectral lines listed in Table 3.2. are used to construct calibration graphs of each element studied.

Table 3.4. Spectral emission lines of the elements studied.

Element	Wavelength (nm)
Na(I)	588.9, 589.6
Ca (II)	393.6, 396.8
Mg (I)	279
Mg(II)	279.5, 280.2
K(I)	766.5

The calibration graphs have been drawn by using solutions from 5 mg/L to 100 mg/L analyte concentration and each point in the graphs represents a signal intensity obtained by averaging 11 consecutive laser pulses. Figure 3.14, 3.15 and 3.16 and 3.17 shows the calibration plots constructed for Ca, Na, Mg and K respectively. In the calibration graphs it can be seen that after 40-50 mg/L analyte concentration the deviation from the linearity occurs. This non-linearity can be explained by the plasma shielding effect (Cremers and Radziemski, 2006) in which the presence of excessive amounts of particles inside the plasma leads to the formation of a thick plasma in which the laser beam cannot penetrate into the particles in the focal volume.

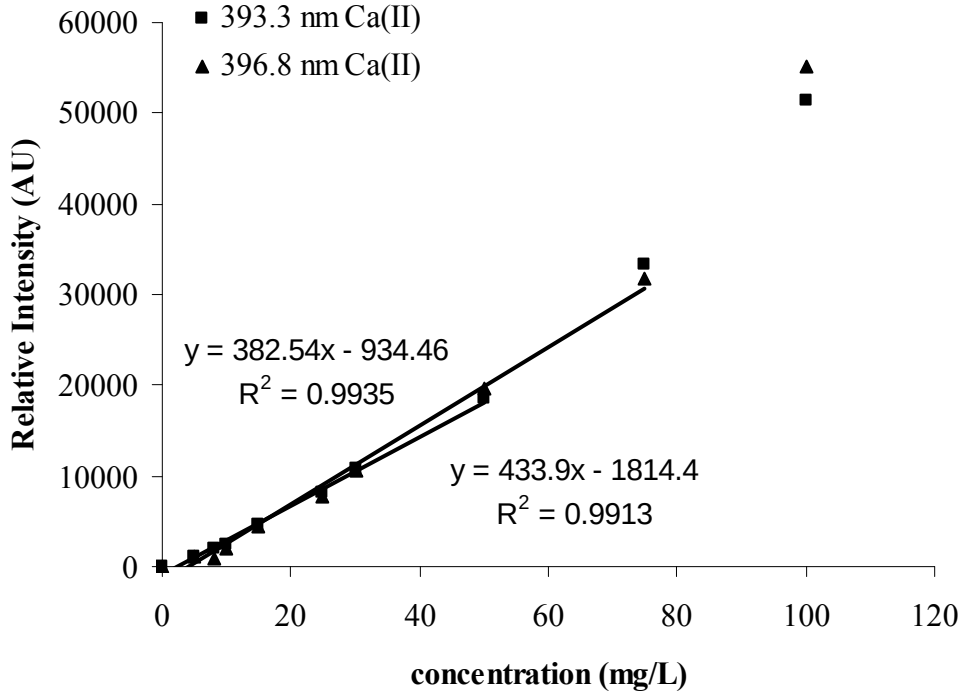

(a)

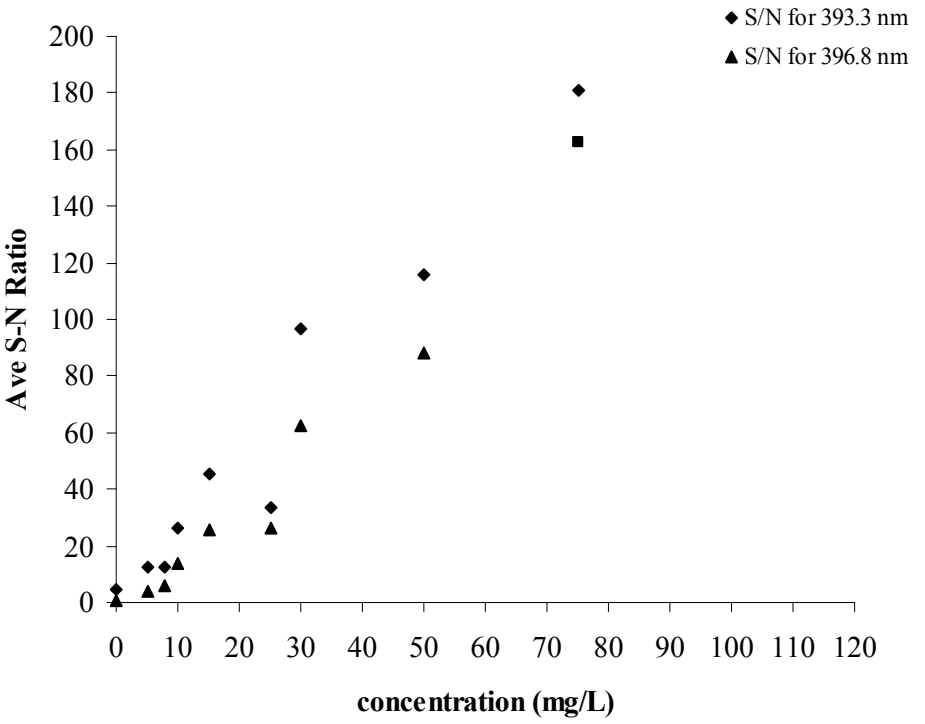

(b)

Figure 3.14. (a) Calibration plot for calcium. (E=80 mJ, t_d=5μs, t_g=10 μs, 10 shot)accumulation) (b) Signal-to-noise trend.

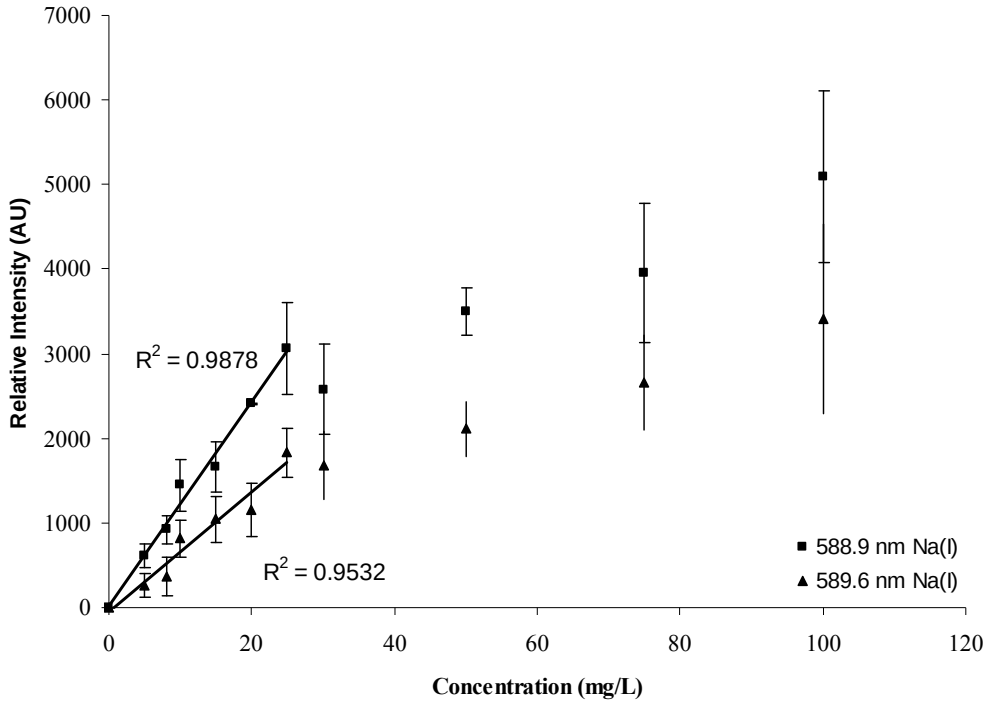

Figure 3.15. Calibration plot for sodium (E=60 mJ, t_d=5μs, t_g =1 ms, 10 shot accumulation).

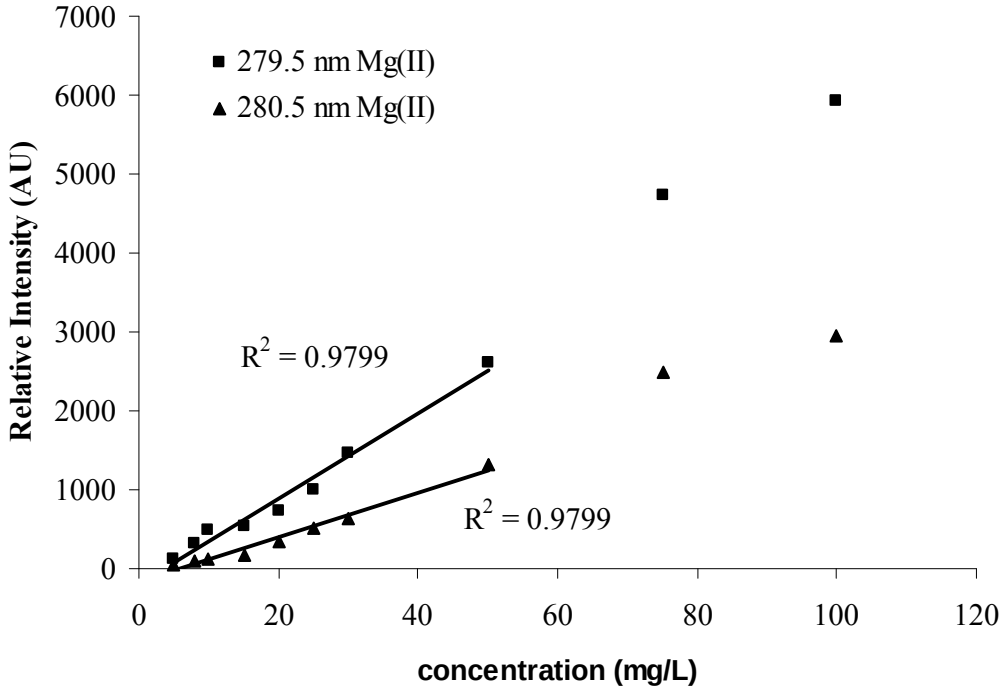

Figure 3.16. Calibration plot for magnesium (E=80 mJ, t_d=5μs, t_g =100μs, 3 shot accumulation.)

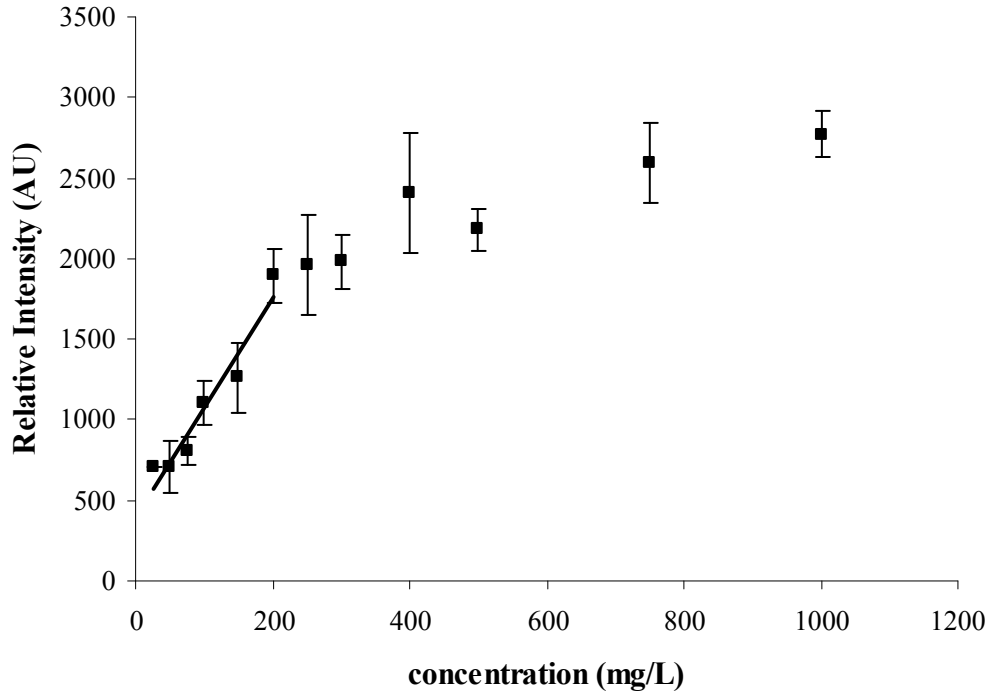

Figure 3.17. Calibration plot for potassium (E=140 mJ, t_d=4μs, t_g =500μs, 10 shot Accumulation).

3.4.1. Detection Limits

The calibration plots have been obtained from the peak heights of the most intense lines of the elements under interest and the detection limits have been calculated by using 3σ method.

$$C = \frac{3\sigma}{m} \qquad 3.2.$$

The detection limit for 588.9 nm sodium line is calculated as 1 mg/L. For magnesium 1.5 mg/L detection limit is calculated as, for 279.5 nm line. For calcium 393.3 nm line, detection limit is 0.6 mg/L. The detection limits and the minimum detectable concentrations are given in Table 3.3. The detection limits have been calculated using the spectra of repetitive mode with accumulation of several spectra so that the precision of the data is more reliable.

Table 3.5. The detection limits and minimum detectable solution concentrations.

Minimum Detectable Concentrations, single shot mode			Detection Limits
	Horizantal Beam	Vertical Beam	Vertical Beam, Repetitive Mode
Na	750 μg/L	250 μg/L	1 mg/L
Ca	1 mg/L	500 μg/L	0.6 mg/L
Mg	2 mg/L	400 μg/L	1.5 mg/L
K	-	10 mg/L	16.3 mg/L

3.4.2. Multi-element Analysis

In order to observe the effect of presence of magnesium and calcium on sodium signal intensity standard solutions of 10 mg/L Ca and 15 mg/L Mg has been added to various sodium concentrations. As it can be seen on Figure 3.19. the presence of magnesium and calcium ions for a given concentrations, do not excessively depress the signal intensity of sodium lines at 588.9 nm and 589.6 nm. Also in Figure 3.20. it is depicted that the presence of Na ions has no drastic effect on magnesium 279.5 nm and calcium 393.3 nm emission lines up to 50 mg/L of sodium concentration. However, after 50 mg/L Na concentration both magnesium and calcium emission intensity decreases.

When a mixture of the four elements aspired into the system, the characteristic peaks have been observed for those elements. Figure 3.19. represents the spectra for the drinking soda and Figure 3.20. for the tap water. These two samples both have high levels of calcium and magnesium. The laser energy has been kept constant at 90 mJ/pulse and delay time as 5 μs and gate width as 1 ms. Ten repetitive shots have been accumulated in the given spectrum. Besides for the quantitative analysis, the signal intensities have been averaged for 20 different spectra. Soda sample has been diluted twenty folds. (the soda sample has been degassed in ultrasonic bath for 5 minutes.) The amount of calcium, sodium, magnesium and potassium present in the mineral water are listed as 257.7, 378.2, 124.3 mg/L respectively on the bottle label (KULA). The analyte signal obtained from the spectra of the mineral water (diluted two times) corresponds to concentrations of 385, 400, 102.5 mg/L respectively.

.

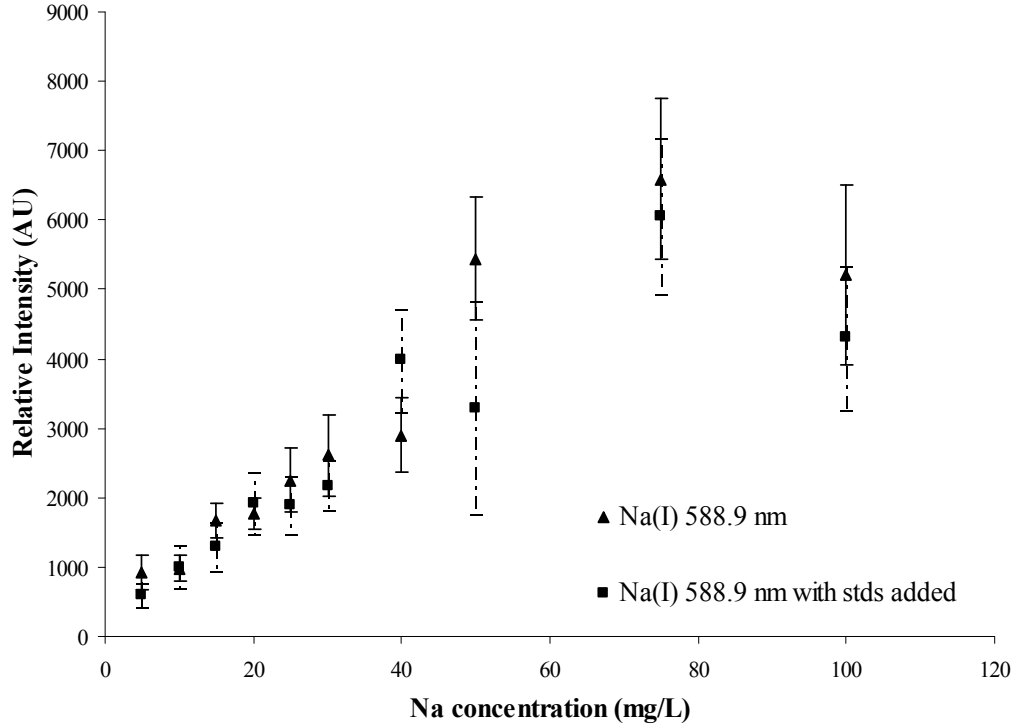

Figure 3.188. (a) The effect of presence of Mg and Ca ions on the signal strength of Na 588.9 nm line.

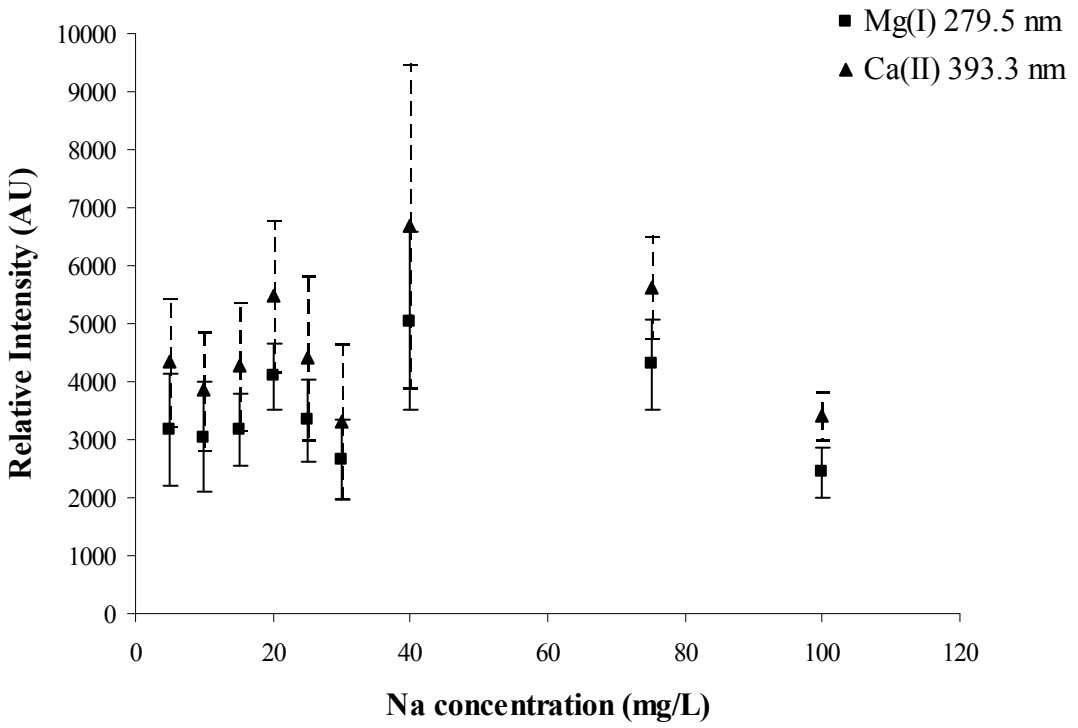

Figure 3.18. (b) Change in intensities of Mg(II) 279.5 nm and Ca(II) 393.3 nm line as Na concentration varies.

3.4.3. Airborne Concentration

When the aqueous solutions are aspired into the system their concentration may be expressed as airborne concentration using Equation 3.1. The abbreviations in the formula stand for the following parameters: c , airborne concentration; Cs, aqueous solution concentration; $r_{n,}$ nebulizer uptake rate; Sr, sample efficiency, r_A carrier gas flow rate; ρ, density of ambient air.

$$c = \frac{Cs * r_n * S_r}{r_A * \rho} \qquad 3.2.$$

Using Equation 3.2, the airborne concentration of the analyte produced by the pneumatic nebulizer may be calculated. The lowest detectable solution concentration for horizontal beam set-up is 750 ppb Na^+ and corresponds to 374 fg/gr air.

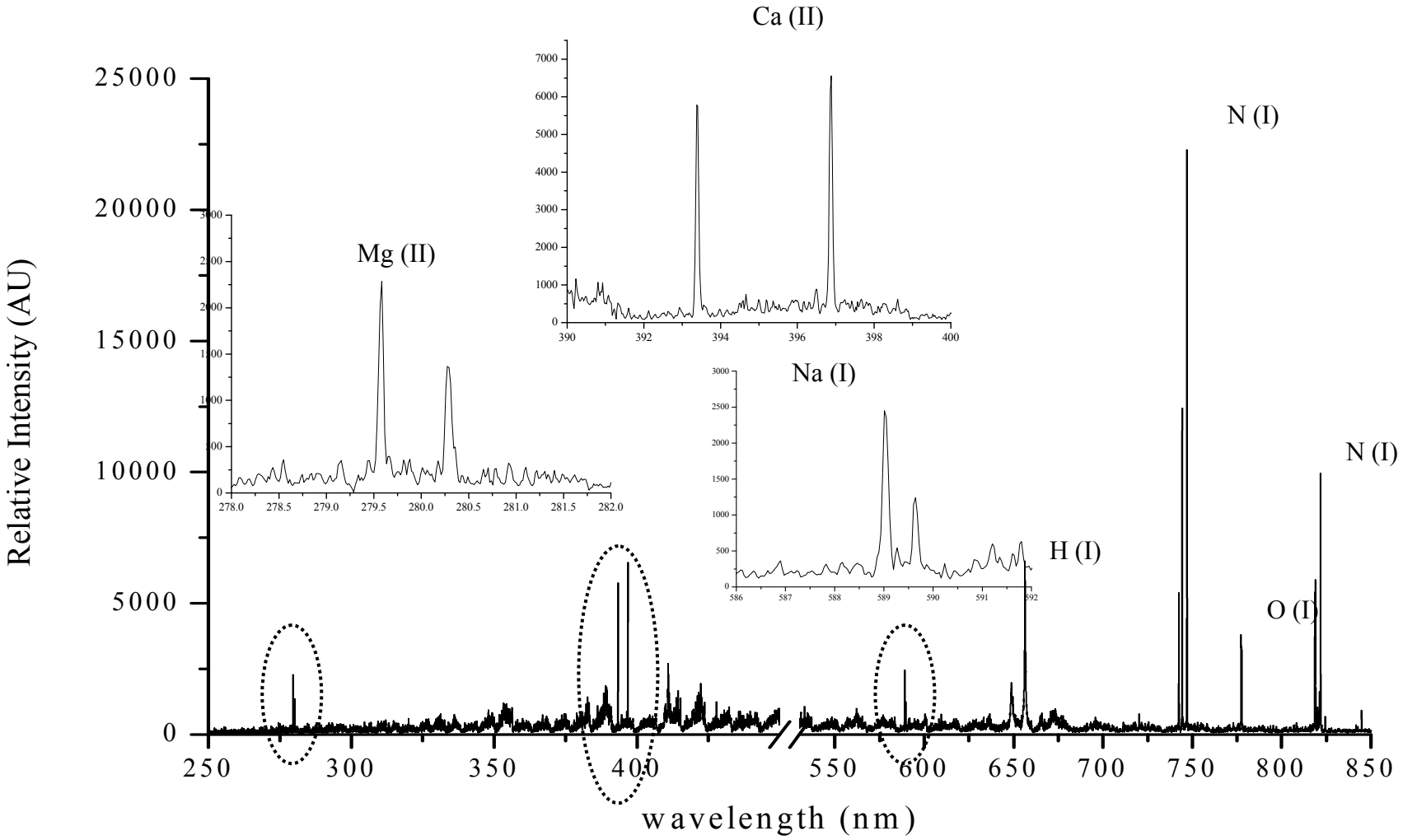

Figure 3.19. Spectra of mineral water (diluted 20 times) (E=90 mJ, td= 5μs tg=1ms, 10 shot accumulation in repetitive mode)

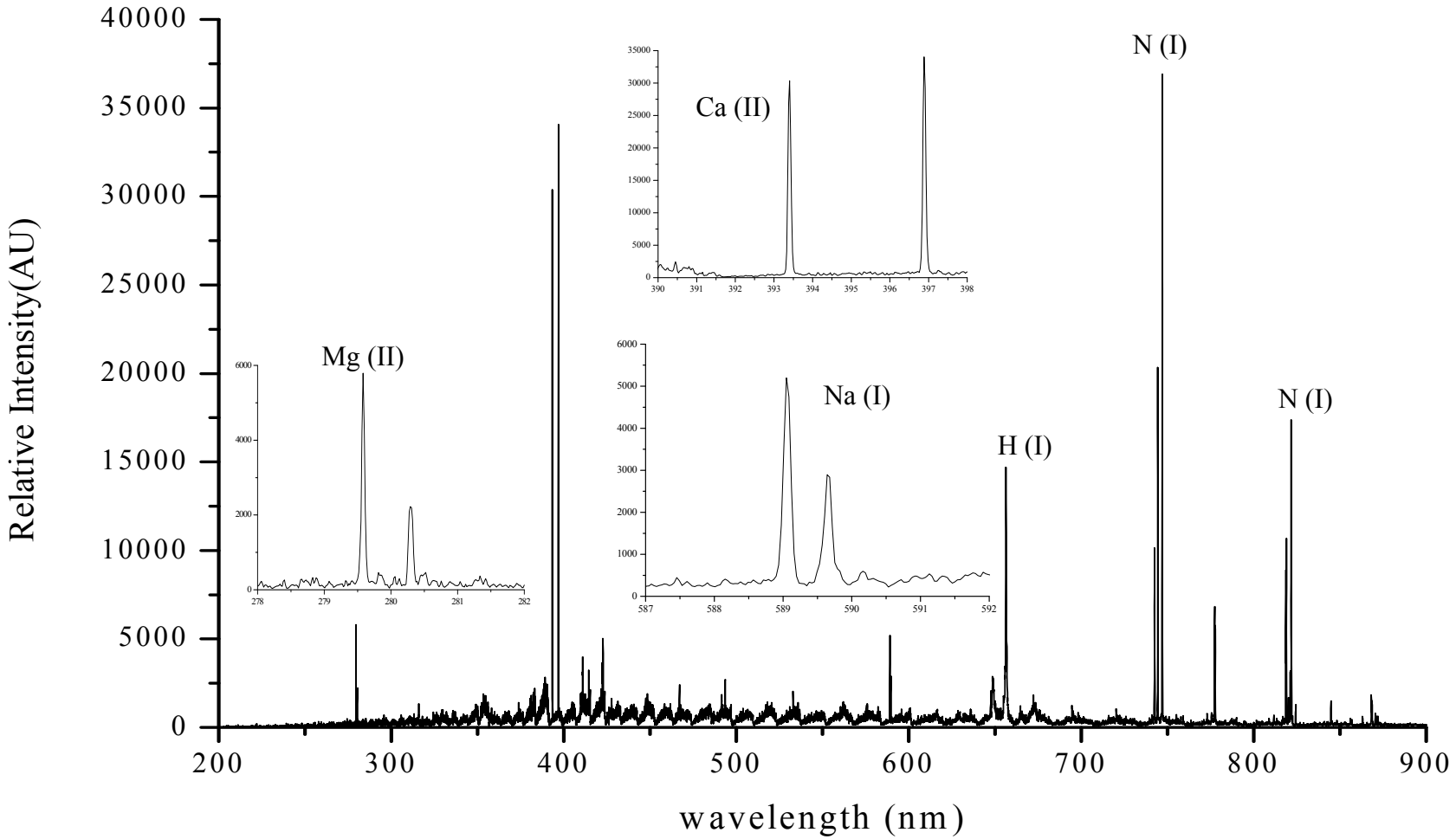

Figure 3.20. Spectra of tap water (E=90 mJ, t_d= 5μs t_g=1ms, 10 shot accumulation in repetitive mode)

48

3.4.3. Particle Size

Particle size measurements of the 100 ppm Na aerosols have been determined using Malvern Mastersizer HD2000. The portable set-up has been attached to the particle size analyzer. The flow of the aerosols has been kept constant and continuous during the measurements. The solution has been carried out with two different air and argon, to see the effect of sample gas density on particle size. When 100 ppm Na solution carried with air the d_{50} of the particles were 1.2 μm in diameter (d_{90}=4.5 μm). Nevertheless, when sample has been carried with argon the d_{50} of the aerosol particles were 1.08 μm (d_{90}=4.3 μm). When the generated aerosols have passed through a single naphion, there has been a decrease observed on the particle size. The 50% of the particles were in range of 0.2 μm (d_{90}= 0.5μm) when carried by air and argon gases. Table 3.4 summarizes the size measurement results. The particle size of aerosols has been decreased by 10 times when membrane dryer has been used. It has been also observed in enhancement of analyte signal.

Table 3.6. Particle size measurements.

Particle Size (d_{90}) (μm)			
without membrane dryer		with membrane dryer	
air	argon	air	argon
4.53	4.29	0.5	0.5

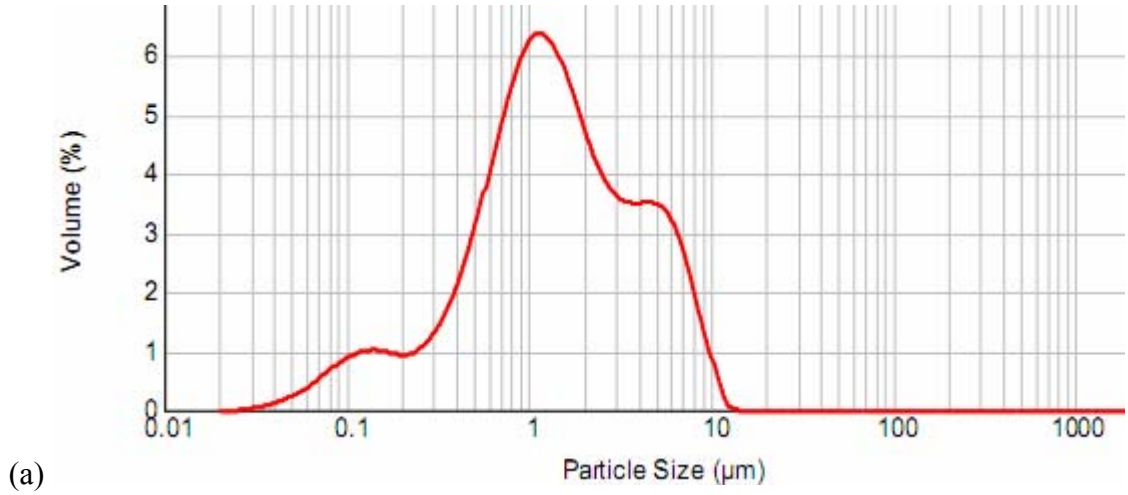

(a)

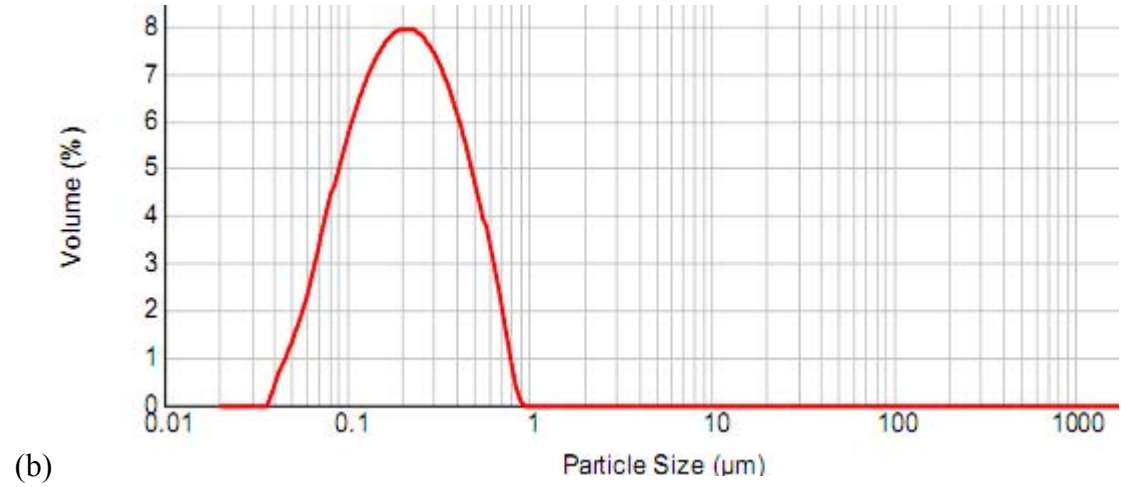

(b)

Figure 3.20. Particle size distribution plots for Na aerosols (a) before passing through membrane dryer (b) after passing through membrane dryer

3.5. Spectral Temperature

Using the Bolztmann Equation given previously in Chapter 1 the plasma temperature was calculated at a specific delay and gate times.

$$\ln\frac{I_1}{I_2} = \ln\frac{g_1 A_1 \lambda_2}{g_2 A_2 \lambda_2} - (E_2 - E_1)/kT \qquad (1.1.)$$

Using the spectra of 100 mg/L sodium solution in aerosol-LIBS system the temperature calculations are done. The 410.995, 493.512, 742.364, 744.229, 746.831, 818.487, 821.634 nm neutral lines of nitrogen are used. The wavelengths are both

observed on spectra and are compatible with the data obtained from literature. (CRC Handbook of Chemistry and Physics', 85th E.)

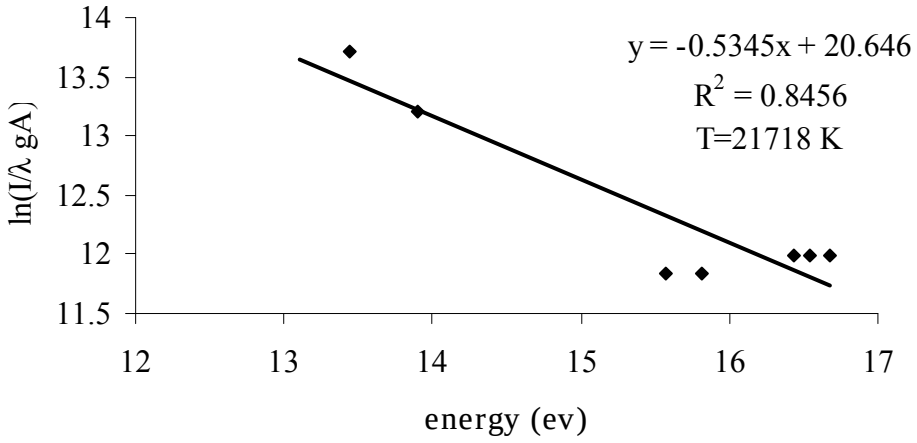

Figure 3.21. The spectral temperature calculation for N(I) lines.

The peak areas of the given nitrogen lines are calculated and substituted into the Bolztman Equation. The slope of the graph shown in Figure 3.22 converted to eV/K, the temperature is found out to be 21718 K when the energy of the incoming beam is 60 mJ and the delay time is 5μs with a gate width of 1ms.

CHAPTER 4

CONCLUSION

In this study, an aerosol generation system has been designed, constructed and coupled to a LIBS system that has been set-up from the commercially available parts. Pneumatic nebulization method has been used to generate particles and a special heating/cooling and membrane drying steps are conjuncted.

Two different experimental LIBS set-up, horizontal and telescopic, were used to form plasma. In telescopic setup, in which the laser beam has been directed from the top of the sample chamber, the plasma image is formed vertically along the slit height of the spectrograph. This way, the variation in plasma position on the slit due to shot to shot variation of the laser pulses has been reduced. The experimental parameters such as flow rate, heating and cooling temperatures, delay times, gate widths, detector gain and laser energies have been optimized for sodium, calcium, magnesium and potassium elements.

Sodium, calcium, magnesium and potassium elements have been studied and the detection limits have been found to be 1, 0.6, 1.5 and 16.3 mg/L respectively. These values for detection limits are comparable to the values given in literature. Besides, real samples mineral water and tap water have been analyzed. Also standard addition of calcium and magnesium on sodium element has shown that the sodium analyte is not highly affected by the presence of the matrix elements.

The efficiency of the heating/cooling unit and the membrane dryer has been demonstrated. 90 % of the aqueous analyte solution has been converted into aerosol. Particle size measurements have been performed. The particles size range has been found as 4.3 μm for sodium. The membrane dryer has reduced the particle size of aerosol droplets to 0.5 μm.

REFERENCES

Aglio M., Colao F., Fantoni R., Lazic V. 2005. Double-pulse LIBS in bulk water and on submerged bronze samples. *Applied Surface Science* 247: 157–162.

Band Yehuda. *Light and Matter*. Wiley, England , 2006.

Caceres J. O., Lopez J. T., Telle H.H., Urena A.G. 2001. Quantitative analysis of trace metal ions in ice using laser-induced breakdown spectroscopy. *Spectrochimica Acta Part B* 56: 831-838.

Cheng M., Martin M. 2000. Detection of Chromium Aerosol Using Time-Resolved Laser-Induced Plasma Spectroscopy. *Applied Spectroscopy* 54: 1279-1285.

Cremers D.A., Radziemski L.J. Handbook of Laser-Induced Breakdown Spectroscopy. John&Willey Sons Ltd. England, 2006.

Gautier C., Fichet P., Menut D., Lacour J., Hermite D. 2004. Study of the double-pulse setup with an orthogonal beam geometry for laser-induced breakdown spectroscopy. *Spectrochimica Acta Part B* 59: 975–986.

Gondal M. A., Hussain T. 2007. Determination of poisonous metals in wastewater collected from paint manufacturing plant using laser-induced breakdown spectroscopy, *Talanta* 71: 73-80.

Griem, H., Haines M. G. Principles of Plasma Spectroscopy. McGraw-Hill, 1964.

Demidov A., Andrews D. An Introduction to Laser Spectroscopy. Springer. 2006.

Hahn D. W., Hohreiter V. 2006. Plasma-Particle Interactions in a Laser-Induced Plasma: Implications for Laser-Induced Breakdown Spectroscopy. *Anal.Chem*. 78: 1509-1514.

Hahn D.W. Carranza J.E. 2001. Aerosol generation systems for development and calibration of laser induced breakdown spectroscopy instrumentation. *Review of Scientific Instruments* 72: 3706-3713.

Hahn D.W. Carranza J.E. 2001. On-line analysis of ambient air aerosols using laser-induced breakdown spectroscopy. *Spectrochimica Acta Part B* 56: 851-864.

Hahn D.W., Asgill M. E. 2009. Particle Size Limits for Quantitative Aerosol Analysis Using Laser-induced Breakdown Spectroscopy: Temporal Considerations. *Spectrochimica Acta PartB* 64: 1153-1158.

Hahn D.W., Diwakar P.K., Jackson P.B. (2007) The effect of multi-component aerosol particles on quantitative laser-induced breakdown spectroscopy: Considerations of localized matrix effects. *Spectrochimica Acta Part B* 62: 1466-1474.

Hahn D.W., Diwakar P.K. Windom B.C. 2006. Dual-pulse Laser Induced Breakdown Spectroscopy for Analysis of Gaseous and Aerosol Systems: Plasma-analyte interactions. *Spectrochimica Acta Part B* 61: 788-796.

Hahn D.W., Lunden M. M. 2000. Detection and analysis of aerosol particles by laser-induced breakdown spectroscopy. *Aerosol Science and Technology* 33: 30-48.

Harith M.A., Charfi B. 2002. *Panoramic laser-induced breakdown spectrometry of water.* Spectrochimica Acta A Part B 57, 1141-1153.

What's naphion? Perma Pure LLC http://www.permapure.com/industry/science/technology/?ind=science (Accessed on June 2010).

Three Four Level Lasers http://www.unc.edu/~dtmoore/3_4level.html (Accessed on June 2010).

Huang J., Liu H., Lin K. 2006. Laser-induced breakdown spectroscopy in analysis of Al+3 liquid droplets: On-line preconcentration by use of flow injection. *Analytica Chimica Acta* 581. 303-308.

Janzen C. Fleige R. Noll R. 2005. Analysis of small droplets with a new detector for liquid chromatography based on laser-induced breakdown spectroscopy. *Spectrochimica Acta Part B* 60: 993-1001.

Koch S., Garen W., Müller M., Neu W. 2004. Detection of chromium in liquids by laser induced breakdown spectroscopy (LIBS). *Appl. Phys A* 79: 1071-1073.

Laserna J.J., Palanco S., Alises A., Cunat J., Baena J. 2003. Development of a portable laser-induced plasma spectrometer with fully-automated operation and quantitative analysis capabilities. *Journal of Analytical Atomic Spectrometry* (18) 933-938.

Laserna J.J., Trujillo L.A., Ferrero A. 2008. Preliminary studies of stand-off laser induced breakdown spectroscopy detection of aerosols. *Journal of Analytical Atomic Spectrometry* 23: 885-888.

Lazic V., Colao F., Fantoni R., Spizzicchino V. 2005. Laser-induced breakdown spectroscopy in water: Improvement of the detection threshold by signal processing. Spectrochimica Acta Part B 60: 1002–1013.

Lazic V., Jovicenic S., Fantoni R., Colao F. 2007. Efficient plasma and bubble generation underwater by an optimized laser excitation and its application for liquid analyses by laser-induced breakdown spectroscopy. *Spectrochimica Acta Part B* 62: 1433–1442.

Lin K., Binke C., Huang J. 2004. Matrix effect on emission current correlated analysis in laser-induced breakdown spectroscopy of liquid droplets. *Spectrochimica Acta Part B* 59: 321–326.

Mohamed Y. Tawfik W. 2008. Improved LIBS limit of detection of Be, Mg, Si, Mn, Fe and Cu in aluminum alloy samples using a portable Echelle spectrometer with ICCD camera. *Optics&LaserTechnology* 40: 30–38.

Molina A., Shaddic C., Sickafoose S., Walsh P. Blevins L. 2005. Effect of temperature and CO2 concentration on laser-induced breakdown spectroscopy measurements of alkali fume. Spectrochimica Acta Part B 60: 1103–1114.

NIST Atomic Spectra Database Lines Form (Accessed on June 2010) http://physics.nist.gov/PhysRefData/ASD/lines_form.html.

Onge L., Kwong E.,Sabsabi M., Vadas E. 2004. Rapid analysis of liquid formulations containing sodium chloride using laser-induced breakdown spectroscopy. *Journal of Pharmaceutical and Biomedical Analysis* 36: 277–284.

Panne U., Neuhausser R. E., Theisen M., Fink H., Niessner R. 2001. Analysis of heavy metal aerosols on filters by laser induced plasma spectroscopy. *Spectrochimica acta Part B* 56: 839-850.

Radziemski L. J., Essien M. 1988. Detection of Cadmium, Lead and Zinc in Aerosols by Laser-induced Breakdown Spectroometry. *Journal of Analytical Atomic Spectrometry* 3: 985-988.

Radziemski L. J., Loree R. T., Cremers D. A., Hoffman N. M. 1983. Time resolved Laser-Induced Breakdown Spectrometry of Aerosols. *Analytical Chemistry* 55: 1246-1252.

Radziemski L.J., Cremers D.A., Loree T.R. 1984. Spectrochemical Analysis of Liquids Using the Laser Spark. *Applied Spectroscopy* 38: 721-729

Unal. S., Yalcin S. 2010. Development of a continuous flow hydride generation laser-induced breakdown spectroscopic system: Determination of tin in aqueous environments. *Spectrochimica Acta Part B* 65: 750–757.

Yaroshchyk P., Morrison R., Body D., Chadwick B. L. 2005. Quantitative determination of wear metals in engine oils using laser-induced breakdown spectroscopy: A comparison between liquid jets and static liquids. *Spectrochimica Acta Part B* 60: 986-992.

Yoshiro I., Nakamura S., Sone K. 1996. Determination of an Iron Suspension in Water by Laser-Induced Breakdown Spectroscopy with Two Sequential Laser Pulses. *Analytical Chemistry* 68: 2981-2986.